SLAC-PUB-589
April 1969
(TH)

HIGH ENERGY PHOTOPRODUCTION AND ELECTROPRODUCTION*

Frederick J. Gilman

Stanford Linear Accelerator Center
Stanford University, Stanford, California

Invited talk given at the
Conference on Particle Interactions at High Energies
at the University of Toronto
March 28-29, 1969

*Work supported by the U. S. Atomic Energy Commission.

I. Introduction

In the next hour I would like to review with you some of the interesting developments, both experimental and theoretical, which have occurred in the past six months to a year in the field of high energy photoproduction and electroproduction. With the advent of SLAC, we have rapidly accumulated a vast amount of new high energy photoproduction data, some of which is summarized[1] in Figure 1. Here we have many of the $\gamma + p \rightarrow$ pseudoscalar meson + baryon differential cross sections which have been recently measured at high energies and we can already see two very striking general features of the data. First of all, $(k_\gamma^{lab})^2 \frac{d\sigma}{dt} \propto (s - M_N^2)^2 \frac{d\sigma}{dt}$ appears to be roughly constant for $k_\gamma^{lab} \geq 3$ GeV/c and $0 \geq t \geq -1\,(GeV/c)^2$ for every pseudoscalar meson + baryon photoproduction process measured. Secondly, although very different at small values of $-t$, beyond $-t \simeq 0.8\,(GeV/c)^2$ every differential cross section seems to be rather smooth, within a factor of three of the others, and fall as roughly e^{3t}. I do not know of any convincing explanation of both of these general features of the data.

II. Pion Photoproduction

In the case of photoproduction of positive pions, the e^{3t} behavior of the differential cross section continues all the way in to $-t \simeq m_\pi^2$, and then $d\sigma/dt$ zooms up by about a factor of two, giving the by now famous forward peak shown clearly in Figures 2 and 3.[2] This forward peak is, perhaps surprisingly, one of the few things that theorists could have predicted in advance of the experiments if we had been a little smarter and if the use of finite energy sum rules (FESR) had been developed a little sooner. To see this,

recall that for photoproduction of single pions there are four amplitudes, which we take to be the four parity conserving t-channel amplitudes F_1, F_2, F_3 and F_4.[3] At $t=0$ there is one kinematic relation among these amplitudes

$$F_2(0) = -(\mu^2/2M_N) F_3(0), \tag{1}$$

which can be satisfied either trivially by both $F_2(0)$ and $F_3(0)$ being zero (a possibility called "evasion" by Regge pole theorists), or by both amplitudes being finite (called "conspiracy"). In the former case, a study of the crossing matrix shows that $\frac{d\sigma}{dt}(t=0)$ vanishes, while in the latter case $\frac{d\sigma}{dt}(t=0)$ is finite and non-zero.

We recall that if an amplitude $A(\nu, t)$ for $\nu > \nu_m$ has the high energy behavior

$$A(\nu, t) \xrightarrow[\nu \to \infty]{} \beta(t) \frac{-1 - e^{-i\pi\alpha(t)}}{\sin \pi \alpha(t)} (\nu/\nu_0)^{\alpha(t)},$$

then we can write the FESR

$$\int_0^{\nu_m} (\nu/\nu_0)^n \operatorname{Im} A(\nu, t)\, d\nu/\nu_0 = \frac{\beta(t)(\nu_m/\nu_0)^{\alpha(t)+n+1}}{\alpha(t)+n+1}, \tag{2}$$

and use low energy data to evaluate the integral over $\operatorname{Im} A(\nu, t)$ on the left hand side in order to predict the Regge parameters on the right hand side. If we do this for the amplitudes $F_2(\nu, t)$ and $F_3(\nu, t)$, we find first of all that the integrals for small t are completely dominated by the nucleon Born terms, with the other low energy resonances and background providing corrections about 20% as large which tend to cancel among themselves. Secondly, the amplitude

F_2, which contains the pion pole, has a rapid variation between $t=0$ and $-m_\pi^2$, while F_3, which involves natural spin-parity exchanges, is slowly varying in the same t interval. The result of all this is a differential cross section which varies rapidly between $t=-m_\pi^2$ and $t=0$ and has the approximate magnitude of the electric Born approximation at $t=0$, which agrees with experiment as we have already seen in Figure 3. In fact, if we note from experiment[2] (see Figure 4) that the effective Regge spin, $\alpha_{eff}(t) \simeq 0$ for $-t \leq 1\,(GeV/c)^2$, then we can develop a "pseudomodel" of π^+ photoproduction where we simply integrate over the low energy data to get the t dependence of the high energy data. This has been done explicitly in a recent paper by Jackson and Quigg[4], who obtain very impressive fits to the high energy data for $-t \leq 0.1\ (GeV/c)^2$ in this way.

Now, previously the sharp forward peak in π^+ photoproduction (as well as $n + p \rightarrow p + n$) has been the main evidence that the pion indulges in what is called an $M=1$ conspiracy, i.e., that the pion gives a non-zero contribution to $F_2(t=0)$, which is able to satisfy the kinematic constraint, Eq. (1), because of the existence of a parity doublet trajectory, π_c, which has $\alpha_{\pi_c}(0) = \alpha_\pi(0)$ and contributes to $F_3(t=0)$. Although there have been a number of good fits to the data with this model[5], including a recent fit of Shih and Tung[6] of $K^+\Lambda$ and $K^+\Sigma$, the idea of an $M=1$ pion trajectory has been in a good deal of trouble during the past year, both theoretically and experimentally[7,8], mainly because via factorization it predicts zeros in various amplitudes which are known not to have them. What the "pseudomodel" does is to show that one can obtain good fits to the data without any assumption of an $M=1$ conspiracy, and in fact Jackson and Quigg, as well as Henyey et al.[9], go on to show that

one can obtain a good fit to the photoproduction data with an evasive pion plus a cut due to absorption corrections[10]. The comparison of their pion plus absorption model for $F_2(t)$ and $F_3(t)$ with the "pseudomodel" is shown in Figure 5, where the "pseudomodel" gives the solid curves (which fit the data very well). How the rapid variation of $F_2(t)$ arises is shown in Figure 6, taken from Henyey et al.[9], where it appears that the slowly varying cut contribution to the amplitude $F_2(\nu, t)$, A, interferes destructively with the rapidly varying evasive pion contribution to $F_2(\nu, t)$, B, to give a total amplitude with a sharp forward peak, M. Thus one can obtain a perfectly good fit to the near forward π^+ photoproduction cross section without an M = 1 pion conspiracy[10].

In the past half year, not waiting for the theorists to catch up, the experimentalists have gone on to more detailed experiments, and have now supplied us with data on the ratio $\frac{d\sigma}{dt}(\gamma + n \rightarrow \pi^- + p)/\frac{d\sigma}{dt}(\gamma + p \rightarrow \pi^+ + n)$ by doing photoproduction on deuterium[11], as seen in Figure 7, as well as experiments with polarized photons for both π^+ and π^- photoproduction[12], as seen in Figures 8 and 9. The π^-/π^+ ratio measures the interference of the amplitudes due to isoscalar photons (G = + 1 exchange) and isovector photons (G = -1 exchange), for if we denote these amplitudes by A^S and A^V respectively, then

$$\frac{d\sigma/dt\,(\gamma + n \rightarrow \pi^- + p)}{d\sigma/dt\,(\gamma + p \rightarrow \pi^+ + n)} = \frac{|1 + A^S - A^V|^2}{|1 + A^S + A^V|^2} \quad . \tag{3}$$

Experiments with linearly polarized photons, on the other hand, select out amplitudes due to the natural spin-parity $(P(-1)^J = +1)$ or unnatural spin-parity $(P(-1)^J = -1)$ exchanges if the photons are polarized perpendicular or

parallel to the production plane, respectively. At high energies the contributions of the two different spin-parity sequences enter the differential cross section incoherently.

Thus if we denote the various possible exchange amplitudes in charged pion photoproduction by:

A_2 if $P(-1)^J = +1$, $G = -1$ (includes quantum numbers of π_c)

ρ if $P(-1)^J = +1$, $G = +1$

π, A_1 if $P(-1)^J = -1$, $G = -1$ $N\bar{N}$ singlet or triplet state

B if $P(-1)^J = -1$, $G = +1$,

then, using an obvious notation, we can write the various cross sections as

$$\gamma_\perp + p \to \pi^+ + n: \quad |A_2 + \rho|^2$$

$$\gamma_\parallel + p \to \pi^+ + n: \quad |\pi + B|^2 + |A_1|^2$$

$$\gamma_\perp + n \to \pi^- + p: \quad |-A_2 + \rho|^2$$

$$\gamma_\parallel + n \to \pi^- + p: \quad |-\pi + B|^2 + |-A_1|^2 .$$

Since we now have data on all these processes, we can go about systematically finding the magnitude of each exchange amplitude. If we do this we find that the data tell us[13]:

1. Very near $t = 0$, only $G = -1$ exchange is required, and we have equal contributions of natural and unnatural spin-parity exchange (e.g., π and π_c in the $M = 1$ conspiracy model). For $-t \gtrsim m_\pi^2$ the unnatural spin-parity (π) contribution falls away and we have dominantly natural spin-parity.

2. There is no interference of π and B seen from $-t = 0$ to $0.6\ (\mathrm{GeV/c})^2$. It is consistent to put $B \simeq 0$ and $A_1 \simeq 0$.

3. A strong interference of A_2 and ρ is needed (or π_c and ρ), including the region $-t \simeq 0.6\ (\mathrm{GeV/c})^2$ where Reggeized ρ exchange is supposed to vanish. Otherwise we cannot explain the small π^-/π^+ ratio in this region. We might take this as possible evidence either for cuts or for additional Regge poles with the ρ's quantum numbers.

As a result of experiments done last summer we also now have a good deal of experimental information on π^o photoproduction at high energy. In Figure 10 we see the various measurements of the differential cross section[14] at high energy, and Figure 11 is the polarized photon data from CEA at 3 BeV.[15] The old Regge model which was used to explain this data involved ω + B exchange[16], but this must be discarded because:

1. The dip at $-t \simeq 0.6\ (\mathrm{GeV/c})^2$, which is expected from the nonsense zero in ω-exchange, is, if anything, filling in as we go to high energy rather than getting deeper as we would expect if we were left at the dip with a B-exchange amplitude which dies away as the energy increases.

2. The polarization data show that even in the dip region where ω exchange is supposed to vanish, we have dominantly natural spin-parity exchange.

3. For $0 \leq -t \leq 1.0\ (\mathrm{GeV/c})^2$ we have $\alpha_{\mathrm{eff}}(t) \simeq 0$ from the $d\sigma/dt$ measurements.

4. Vector dominance arguments suggest that near the dip one has dominantly $G = -1$ (from isovector photons) exchange[17].

Thus again we have a good case for cuts or at least additional Regge trajectories, this time with the quantum numbers of the ω. A recent paper by Capella and Tran Tranh Van[18], in fact, gets good agreement with both the differential cross section and polarization measurements using a model based on ω plus ω-Pomeron cut exchange.

The past few months have also given us our first look at the process $\gamma + p \to \pi^- + \Delta^{++}$ at high energy[19]. As shown in Figures 12 and 13 the differential cross sections for this process have the remarkably property of being essentially degenerate with the $\gamma p \to \pi^+ n$ cross sections for $-t \geq 0.2\ (\mathrm{GeV/c})^2$, while for smaller values of $|-t|$ they increase like e^{12t} until $-t \simeq m_\pi^2 = 0.02\ (\mathrm{GeV/c})^2$, whereupon they drop as $t \to 0$. How does one explain this final dip instead of the peak observed in $\gamma + p \to \pi^+ n$? Within the framework of models with cuts[10] there is a plausible explanation, although I know of no specific detailed calculations within such models of $\gamma p \to \pi^- \Delta^{++}$. There are in fact two "explanations". The first one is that in one of the forward amplitudes the cut, instead of interfering destructively with the vanishing pion contribution at $t \to 0$ as in $\gamma + p \to \pi^+ + n$, interferes constructively with the "evasive" pion amplitude and thus produces a dip as $t \to 0$. This explanation is very unlikely if one has a physical picture of cuts as arising from absorptive corrections in which case the interference should be destructive. Alternately, since there are two independent forward amplitudes for $\gamma p \to \pi^- \Delta^{++}$ instead of the single forward amplitude for $\gamma p \to \pi^+ n$, we could have the vanishing pion contribution in one of the amplitudes and a relatively constant cut contribution in the other, so that in the differential cross section which is the sum of their squares we again have a resulting forward dip. This latter explanation is certainly the more likely one.

III. The Vector Dominance Model for Pion Photoproduction

One of the minor theoretical industries of the last couple of years has been gathering together the photoproduction data and comparing it with the data on ρ production by pions in order to test vector dominance. Up to the time of the Vienna conference things looked very good. For example, in Figure 14 we show the comparison[11, 20] with experiment of the relation[21]:

$$\frac{1}{2}\left[\frac{d\sigma}{dt}(\gamma p \to \pi^+ n) + \frac{d\sigma}{dt}(\gamma n \to \pi^- p)\right]$$

$$= g^2_{\gamma\rho}\ \rho^{hel}_{11}\ \frac{d\sigma}{dt}(\pi^- p \to \rho^o n) + g^2_{\gamma\omega}\ \rho^{hel}_{11}\ (\pi^- p \to \omega n). \qquad (4)$$

Here $g_{\gamma\rho} = \frac{e}{f_\rho} = \frac{e}{2\gamma_\rho}$ is the rho-photon coupling constant, $g_{\omega\gamma}$ is the omega-photon coupling constant, and ρ^{hel}_{11} is the helicity + 1 density matrix element of the vector meson. Because we have taken the sum of neutron and proton photoproduction cross sections, we have eliminated the isoscalar-isovector photon or corresponding $\rho - \omega$ interference terms in the differential cross sections. Then, in as much as $g^2_{\gamma\omega} \simeq \frac{1}{9}\ g^2_{\gamma\rho}$ and the not very well known ω production differential cross sections appear to be definitely smaller than the corresponding ρ cross sections, we can safely neglect the second term on the right hand side. Thus we get the comparison with experiment[20] shown in Figure 14, which is rather impressive in shape and in absolute magnitude if we use $\gamma^2_\rho/4\pi \simeq 0.5$.

What has happened in the past few months is that the polarized photon data has come along and enabled us to make a much more sensitive test of the vector dominance model (VDM). If we write $\sigma^{\pm}_{\perp}$ and $\sigma^{\pm}_{\parallel}$ as the photoproduction cross sections for $\pi^{\pm}$ mesons produced by photons with

polarization perpendicular and parallel, respectively, to the reaction plane, then we have the two relations:

$$\frac{1}{2}(\sigma_{\perp}^{+} + \sigma_{\perp}^{-}) = g_{\gamma\rho}^{2}(\rho_{11}^{hel} + \rho_{1-1}^{hel})\frac{d\sigma}{dt}(\pi^{-}p \to \rho^{o}n)$$

$$\frac{1}{2}(\sigma_{\parallel}^{+} + \sigma_{\parallel}^{-}) = g_{\gamma\rho}^{2}(\rho_{11}^{hel} - \rho_{1-1}^{hel})\frac{d\sigma}{dt}(\pi^{-}p \to \rho^{o}n), \tag{5}$$

where we again have dropped the negligible ω production term. The sum of Eqs. (5)gives the previous relation, Eq. (4), while the difference divided by the sum gives

$$A(\pi^{+} + \pi^{-}) = \frac{(\sigma_{\perp}^{+} + \sigma_{\perp}^{-}) - (\sigma_{\parallel}^{+} + \sigma_{\parallel}^{-})}{(\sigma_{\perp}^{+} + \sigma_{\perp}^{-}) + (\sigma_{\parallel}^{+} + \sigma_{\parallel}^{-})} = \frac{\rho_{1-1}^{hel}}{\rho_{11}^{hel}} \quad . \tag{6}$$

The comparison[22] of this relation with experiment is shown in Figure 15, and we see that the agreement between Eq. (6) and experiment is very poor. The first reaction of many theorists to this is naturally to look for what could be wrong with the experiments. The main input to the left hand side of Eq. (6) comes from the DESY polarized photon data[12], and we recall from Section II that just outside the forward peak in either π^{+} or π^{-} photoproduction they show $\sigma_{\perp} >> \sigma_{\parallel}$ (recall Figures 8 and 9). This is in excellent agreement with the almost model independent predictions (the pseudomodel of Jackson and Quigg[4]) based on the low energy data and finite energy sum rules, so it is very unlikely that the polarized photon data is grossly wrong. This brings our attention to the ρ density matrix elements on the right hand side of Eq. (6) where one might well worry about questions

of interfering background in the rho meson signal in $\pi^- p \to \pi^+ \pi^- n$ which could make the determination of the density matrix elements unreliable. One can only say that this question has been looked at by several groups of people[20,23], and by taking various mass cuts they get the same answer; namely that ρ^{hel}_{1-1} at $t = -0.2$ and $t = -0.4$ $(GeV/c)^2$ is small and negative, which makes the right hand side of Eq. (6) small and negative while the left hand side is decidedly positive and greater than or equal to 0.4.

Another way out has been suggested by Bialas and Zalewski[24] who say that the VDM is not wrong unless one cannot find <u>any</u> frame with z axis in the scattering plane for the final vector meson in which the relations (5) hold. They then rotate about the normal to the production plane until they get to the Donohue-Hogaasen frame[25] where the second of relations (5) seems to work[24]. While I do not understand this point of view, one may still be interested to see if such a rotation of frames can patch up the discrepancy. Since rotating about the normal to the production plane does not change the first of the relations in Eq. (5) we compare it alone with experiment in Figure 16.[26] We see a factor of two to three discrepancy out to $-t \simeq 0.4$ $(GeV/c)^2$, so that the agreement is still poor.

Basically, the discrepancy arises because the polarized photon data tell us that photoproduction proceeds dominantly through natural spin-parity exchanges, while the ρ density matrix indicates roughly equal amounts of natural and unnatural spin-parity exchange for this process. Thus, unless one can show that the ρ density matrix elements are very much different than what the presently available experiments indicate, <u>the dynamics of the two processes appear to be different</u> and no amount of juggling of frames or scale factors can change that and make the agreement good.

There have also been a few other recent tests of the VDM. If we are willing to make the additional assumption that the magnitude of $d\sigma/dt$ for $\gamma + N \to \pi + \Delta$ does not change under $s \longleftrightarrow u$ crossing (which would be true if only Regge trajectories of one signature were exchanged), then we have

$$\frac{d\sigma}{dt}(\gamma + p \to \pi^- + \Delta^{++}) = \frac{d\sigma}{dt}(\pi^+ + p \to \gamma + \Delta^{++}) \tag{7}$$

and now we can use the VDM to obtain,

$$\frac{1}{2}\left[\frac{d\sigma}{dt}(\gamma + p \to \pi^- + \Delta^{++}) + \frac{d\sigma}{dt}(\gamma + n \to \pi^+ + \Delta^-)\right]$$

$$= g^2_{\gamma\rho}\, \rho^{hel}_{11}\, \frac{d\sigma}{dt}(\pi^+ p \to \rho^o \Delta^{++}) \,. \tag{8}$$

We have again dropped an ω production cross section which is negligible out to moderate values of t. Figure 17 again shows a disagreement by a factor of two to three[27].

A similar disagreement is found if we take the data[28] for $K^- p \to \rho^- \Sigma^+$ at 5.5 GeV/c, assume $I = 1/2$ exchange to relate this to $K^- p \to \rho^o \Sigma^o$, assume $s \longleftrightarrow u$ crossing does not change the magnitude of $d\sigma/dt$ to relate this to $\rho^o p \to K^+ \Sigma^o$, and then use the VDM to compare with $\gamma p \to K^+ \Sigma^o$. At $t = -0.4$ (GeV/c)^2 the disagreement is by a factor of ten, and the isoscalar part of the photon might give us a helpful factor of two, but not much more[29]. In both these tests of VDM, however, we have the $s \longleftrightarrow u$ crossing assumption to put the blame on, while the single pion photoproduction tests are independent of any such assumption and leave little room to avoid the discrepancy between theory and experiment discussed above.

IV. Sign of the $\pi^o \to \gamma\gamma$ Decay Amplitude

Before leaving the subject of single pion photoproduction on such a gloomy note, I would like to indicate one way in which some of the high energy data we have acquired is useful in other connections; in this case, in determining the sign of the $\pi^o \to \gamma\gamma$ amplitude. The $\pi^o \to \gamma\gamma$ amplitude is defined by

$$S_{\gamma\gamma \to \pi o} = (2\pi)^4 \delta(q - k_1 - k_2) \frac{1}{\sqrt{8 q_0 k_{10} k_{20}}} \epsilon_{\mu\nu\lambda\sigma} \epsilon^{(1)}_{\lambda} \epsilon^{(2)}_{\nu} k_{1\lambda} k_{2\sigma} F(q^2). \quad (9)$$

In perturbation theory, the triangle diagram with a proton going around the closed loop gives $F(0) = -e^2 g_{\pi NN}/4\pi^2 M_N$. In general, $F(0)$ is proportional to a weighted average of the squares of the charges of the fermions in the loop. All this is of some current interest because of the work of Adler[30], who has shown that the PCAC equations for the neutral members of the axial-current octet must be modified by an additional term arising from exactly these same closed fermion loop triangle diagrams. This additional term then gives a definite, non-zero, prediction for the $\pi^o \to \gamma\gamma$ amplitude. The sign and magnitude of this amplitude is then sensitive to what model of elementary particles you use in the triangle graphs. Now we can get our hands on the sign experimentally by noting that one observes constructive interference between the Primakoff effect and the rest of the amplitudes involved in π^o photoproduction[31], as shown in Figure 18, where the solid line (dashed line) is what one expects for constructive (destructive) interference. Using FESR's, we may translate this experimental observation into a statement that eF and $-eg_{\pi NN}$ have the same sign[32], in agreement in sign (and also magnitude) with the results of perturbation theory with a single proton loop!

V. Vector Meson Photoproduction

Let us now turn to a very different subject area, that of vector meson photoproduction, and in particular ρ photoproduction from nuclei. In the recent issues of Physical Review Letters, two new experiments have been reported on $\gamma A \rightarrow \rho A$, one at Cornell[33] at 6.2 GeV/c, and one at SLAC[34] at 8.8 GeV/c. From these measurements one can extract two important numbers, the ρN total cross section, $\sigma_{\rho N}$, and within the context of the VDM, the $\gamma-\rho$ coupling constant, $g_{\gamma\rho} = e/f_\rho = e/2\gamma_\rho$. The first number, $\sigma_{\rho N}$, may be obtained from observing the relative A dependence of $\frac{1}{A}\frac{d\sigma}{dt}(t = t_{min}, A)$, together with a model of the nuclear density to use in calculating the absorption of rhos by the nuclear matter. In this way (see Figure 19) SLAC obtains $\sigma_{\rho N} = 30\ ^{+6}_{-4}$ mb, while Cornell obtains $\sigma_{\rho N} = 38.5 \pm 4.5$ mb, using somewhat different nuclear models, but with the same experimental A dependence. Given a value of $\sigma_{\rho N}$, then an absolute measurement of $\frac{d\sigma}{dt}(t_{min}, A)$ on any nucleus gives $\gamma_\rho^2/4\pi$. A heavy nucleus like Pb is better for this since it will be rather "black" no matter what $\sigma_{\rho N}$ is and hence the calculated value of $\frac{d\sigma}{dt}$ will not depend strongly on the exact value of $\sigma_{\rho N}$ as shown in Figure 19. From their data, SLAC obtains $\gamma_\rho^2/4\pi = 1.1 \pm 0.2$ and Cornell, $\gamma_\rho^2/4\pi = 1.1 \pm 0.15$, in disagreement with the older value from DESY[35] of 0.45 ± 0.1 and the value from the colliding rings[36], 0.52 ± 0.03, when the ρ rather than the photon is on its mass shell.

Is $\gamma_\rho^2/4\pi \simeq 0.5$ or $\simeq 1.0$ on the photon mass shell? If we look at Figure 20[37], we see what appears to be good evidence from many places that $\gamma_\rho^2/4\pi \simeq 0.5$ on the photon mass shell. A closer look, however, reveals not such a clear picture. Numbers 3, 4 and 8 are in some doubt because of the

discrepancy with the VDM for polarized photons we discussed earlier. Number 7 should probably not be trusted to better than a factor of two in any case, since, aside from questions of the validity of the VDM for single pion photoproduction, it involves subtracting data from several different bubble chamber experiments. Number 2 implicitly assumes, in dispersion theory language, that the pion charge form factor obeys an unsubtracted dispersion relation which is dominated for $q^2 \simeq 0$ by the rho meson. This allows one to obtain the relation $\gamma_\rho = \gamma_{\rho\pi\pi}$ from the normalization of the charge form factor at $q^2 = 0$, $F_\pi(0) = 1$, and then use the $\rho \to \pi\pi$ width to get $\gamma_{\rho\pi\pi}$ and hence γ_ρ. This may or may not be correct since (1) a priori one does not know if such an unsubtracted dispersion relation for a charge form factor is correct, and (2) judging from the radius of either $F_1^V(q^2)$ or $G_E^V(q^2)$ it appears that such an unsubtracted dispersion relation dominated by the rho meson near $q^2 = 0$ is not the case for either choice of the nucleon's charge form factors.

Number 6 leads to $\left[(\gamma_\rho^2/4\pi)(\gamma_{\rho\pi\pi}^2/4\pi)\right]^{-1} = 2.1 \pm 0.2$ using the Gell-Mann-Sharp-Wagner model[38] for ω decay and the present values[39] for $\Gamma(\omega \to \pi\gamma)/\Gamma(\omega \to 3\pi)$. If we assume $\gamma_\rho = \gamma_{\rho\pi\pi}$ we get $\gamma_\rho^2/4\pi = 0.7 \pm 0.1$, but if we put in $\gamma_{\rho\pi\pi}^2/4\pi = 0.5 - 0.6$ from the ρ-width, then we have $\gamma_\rho^2/4\pi \simeq 0.9 \pm 0.1$. Thus we are left with Numbers 1 (if we believe certain experimental results on $\sigma_{\gamma\rho}$ and $\frac{d\sigma}{dt}(\gamma + p \to \rho^o + p)_{t=0}$) and 5 as showing that $\gamma_\rho^2/4\pi \simeq 0.5$ on the photon mass shell, while Cornell and SLAC get $\gamma_\rho^2/4\pi \simeq 1.0$.

I have frankly gone through the list in Figure 20 in a very critical way, perhaps more so than many of the individual entries deserve. But my main point is not that almost every entry is doubtful in one way or another, but that we should all be a little more careful in accepting too quickly certain

experimental results because they fit a preconceived notion of what we might expect them to be.

Taking at face value the Cornell and SLAC value of $\gamma_\rho^2/4\pi \simeq 1.0$ on the photon mass shell, while the colliding beams give $\gamma_\rho^2/4\pi \simeq 0.5$ on the rho mass shell, what can we do to fix the troubles with the VDM we find here also? Theoretically there are a number of paths open to us, such as a q^2 dependence of γ_ρ, additional vector mesons, and/or hadronic form factors to make the cross sections or amplitudes for zero-mass rhos different from those of rhos on the mass shell. To help us in choosing among the various paths we can, and should, do certain further experiments. First of all, it will be interesting to get the $d\sigma/dt$ measurements of SLAC on H_2 at 9 GeV/c to check $d\sigma/dt = (e/2\gamma_\rho)^2\, \sigma_{\rho N}^2/16\pi$ at their energy, as well as their data at 16 GeV/c. Second, one should look hard for higher mass vector mesons, which may be invoked to cure some of the difficulties of vector dominance, as had been done by various people, including several[40] here at Toronto. Third, it will be interesting to study both the energy and A dependence of photon-nucleus total cross sections[41] and to thus observe the increased shielding (shown in Figure 21) at higher energies due to the diffractive production of vector mesons, which changes the A dependence of $\sigma_T(\gamma A)$ from being proportional to A toward being proportional to $A^{2/3}$, as expected for hadronic-nuclear cross sections at high energies.

VI. Multibody Photoproduction

I would like to note one more kind of photoproduction experiment, which is just beginning. These are the multibody photoproduction processes;

a first analysis of the results of a bubble chamber exposure to the monochromatic photon beam at SLAC (from e^+ annihilation) has recently come out[42]. In addition to clear signals for $\gamma p \to \rho^o p$, $\gamma p \to \omega p$, $\gamma p \to \pi \Delta$, $\gamma p \to \rho \Delta$, etc., a great proliferation of other resonant final states such as $\pi\rho\Delta$, $\pi\omega\Delta$, etc. has been found. This promises to be a very rich area of research in the near future.

VII. High Energy Electroproduction

By now everyone here should be completely familiar with the kinematics of electroproduction where one detects only the final electron: If the incident electron has energy E and the final electron energy E' then the electroproduction experiments can be summarized in two structure functions, W_1 and W_2, which depend on the two variables $\nu = q_0 = E - E'$ and q^2, the energy and four-momentum squared of the virtual photon. The connection between the cross-section for scattering into a given final electron energy, E', and angle, θ, and the functions W_1 and W_2 is[43]

$$\frac{d^2\sigma}{d\Omega dE'} = \frac{4\alpha^2 E'^2}{q^4}\left[2\sin^2\theta/2\ W_1(\nu, q^2) + \cos^2\theta/2\ W_2(\nu, q^2)\right]. \tag{10}$$

The only other bit of kinematics I wish to note is that if we wish to relate W_1 and W_2 to total photoabsorption cross sections for virtual photons, then we have for large ν and fixed q^2 that[44]

$$\begin{aligned} \nu W_2 &\to q^2(\sigma_T + \sigma_S) \\ W_1 &\to \nu\,\sigma_T\ , \end{aligned} \tag{11}$$

where $\sigma_T(\nu, q^2)$ and $\sigma_S(\nu, q^2)$ are the total cross sections for transversely and longitudinally polarized virtual photons, respectively.

It was originally suggested by Bjorken[45] that one may have a possible universal form as $\nu, q^2 \to \infty$

$$\nu W_2 \to F_2(\nu/q^2)$$
$$W_1 \to F_1(\nu/q^2) , \tag{12}$$

which is supported for νW_2 by the 6^o data shown in Figure 22.[46] The original motivation for such a universal form came from models where the nucleon is made out of point-like constituents which interact with the virtual photon in a regime (infinite momentum frame, large ν and q^2) where the impulse approximation is valid for the interaction of the photon with the constituents of the nucleon. Such a picture, as developed by Bjorken[47] (originally with constituents called quarks) and by Feynman[48] (with constituents called "partons"), does indeed lead naturally to a universal form for νW_2. Some recent work on such constituent models has been done at SLAC by Bjorken and Paschos[49].

More recently there has been a shift in the theoretical emphasis of preprints on this subject to models which are essentially of a diffraction or multiperipheral type, or in other words involve Pomeranchukon exchange. The first paper along these lines that I know of is that of Harari[50]. The motivation for such a theory is the flatness of the experimental curve (see Figure 22) for $\nu W_2(\nu, q^2)$ (recall from Eq. (11) that this means a constant total cross section at fixed q^2) all the way down to $\nu/q^2 \simeq 2$, and that the resonance bumps all seem to be going away rapidly as q^2 increases. Some

recent papers in this general category are by Abarbanel, Goldberger and Treiman[51]; Drell, Levy and Yan[52]; and by Sakurai[53].

Although these two types of theories are not necessarily in conflict with one another, they do emphasize different aspects of the subject. The constituent models easily yield a universal form for νW_2, but have trouble in explaining the flatness of the observed νW_2 vs. ν/q^2 curves. On the other hand, the diffraction models have no trouble explaining the flatness of the curves for νW_2, being motivated by it in the first place, but the universal form for νW_2 has to be imposed a posteriori.[54]

There are two types of experiments which will help us in choosing between theories. First is electroproduction off neutrons, since diffraction models say that the neutron and proton cross sections should be the same, while constituent theories say in general that they are different (depending of course on the constituents). Second is the separation of σ_T and σ_S, or equivalently W_1 and W_2. In constituent models we expect that at large q^2 $\sigma_T >> \sigma_S$ ($\sigma_S >> \sigma_T$) if the constituents interacting with the photon are fermions (bosons). As for diffraction models, the separation of σ_T and σ_S will permit us to make a critical test of models such as Sakurai's which make specific predictions of σ_S/σ_T.[53] The beginnings of a separation of σ_S and σ_T, at least, we can expect to see accomplished in the next few months.

References and Footnotes

1. R. Diebold, unpublished. I would like to thank Dr. Diebold for the use of several of his unpublished figures, particularly Figures 1 and 17, and for discussions about parts of this talk.
2. A. M. Boyarski et al., Phys. Rev. Letters 20, 300 (1968); and the rapporteur's talk of B. Richter in Proceedings of the Fourteenth International Conference on High Energy Physics, Vienna, Austria, 1968 (CERN Scientific Information Service, Geneva, Switzerland, 1968), p. 3.
3. See, for example, the paper of J. S. Ball, W. R. Frazer and M. Jacob, Phys. Rev. Letters 20, 518 (1968) for the definitions of these amplitudes.
4. J. D. Jackson and C. Quigg, Berkeley preprint, UCRL-18764 (1969) unpublished.
5. See, for example, the fits by J. S. Ball, W. R. Frazer and M. Jacob, Ref. 3, and by F. S. Henyey, Phys. Rev. 170, 1619 (1968).
6. C. C. Shih and W. K. Tung, preprint, October, 1968 (unpublished).
7. Theoretically, the arguments of S. Mandelstam, Phys. Rev. 168, 1884 (1968), which provide a connection between an M = 1 pion and the current algebra results for soft pions, also lead on closer examination to the vanishing of certain amplitudes for hard pions, contradicting experiment; S. Mandelstam, unpublished, and R. F. Sawyer, Phys. Rev. Letters 21, 764 (1968). Models which can get around this difficulty with an M = 0 pion plus an M = 1 "pion" and "pion-conspirator" have been constructed by R. Blankenbecler and R. Sugar, Phys. Rev. Letters 20, 1014 (1968), and by W. R. Frazer, H. M. Lipinski, and D. R. Snider, Phys. Rev. 174, 1932 (1968).
8. Experimentally we have the absence of the zero at $t = 0$ in $\pi p \to \rho \Delta$ predicted by M. LeBellac, Phys. Letters 25B, 524 (1967); see M. Aderholz et al., Phys. Letters 27B, 174 (1968).

9. F. S. Henyey, G. Kane, J. Pumplin and M. Ross, University of Michigan preprint, 1968 (unpublished).

10. Presumably whatever one can presently fit with an M = 0 pion plus a cut can also be fit just as well by an M = 0 pion plus an M = 1 "pion" and "pion-conspirator", with the cut being imitated by the M = 1 "pion" and "pion-conspirator" poles, and vice versa. See the models of Blankenbecler and Sugar and Frazer, Lipinski and Snider, Ref. 7, in connection with the latter, Regge-poles-only, model.

11. A. M. Boyarski et al., Phys. Rev. Letters 21, 1767 (1968).

12. C. Geweniger et al., Phys. Letters 28B, 155 (1968); and data of C. Geweniger et al., and Z. Bar-Yam et al. quoted in B. Richter's rapporteur talk, Ref. 2.

13. R. Diebold, Phys. Rev. Letters 22, 204 (1969).

14. M. Braunschweig et al., Phys. Letters 26B, 405 (1968); R. Anderson et al., Phys. Rev. Letters 21, 384 (1968).

15. D. Bellenger et al., to be published and quoted in B. Richter's rapporteur talk, Ref. 2.

16. J. P. Ader, M. Capdeville, and Ph. Salin, Nucl. Phys. 33, 407 (1967).

17. H. Harari, Phys. Rev. Letters 21, 835 (1968).

18. A. Capella and J. Tran Tranh Van, Orsay preprint, 1968 (unpublished).

19. A. M. Boyarski et al., Phys. Rev. Letters 22, 148 (1969).

20. R. Diebold and J. A. Poirier, Phys. Rev. Letters 20, 1532 (1968).

21. See, for example, D. S. Beder, Phys. Rev. 149, 1203 (1966); H. Joos, Acta Phys. Austriaca, Suppl. No. IV, 320 (1967).

22. R. Diebold and J. A. Poirier, Phys. Rev. Letters 22, 255 (1969).

23. L. J. Gutay et al., Phys. Rev. Letters 22, 424 (1969).

24. A. Bialas and K. Zalewski, Phys. Letters 28B, 436 (1969).

25. J. T. Donohue and H. Hogaasen, Phys. Letters 25B, 554 (1967).

26. R. Diebold and J. A. Poirier, preprint, SLAC-PUB-569, 1969 (unpublished).

27. R. Diebold, private communication. We must also be careful here about the normalization of the cross sections for $\pi^- p \to \rho^0 \Delta^{++}$ since there are two fairly broad resonances in the final state, making a determination of the absolute normalization of the cross section both experimentally and theoretically somewhat ambiguous.

28. U. E. Kruse et al., University of Illinois preprint, 1968 (unpublished).

29. F. J. Gilman (unpublished). M. Davier, SLAC-PUB-514, 1968 (unpublished) has also tried to test the VDM for $K^+\Lambda$ photoproduction using the total cross sections for $K^- p \to \rho\Lambda$, $K^- p \to \omega\Lambda$, and $K^- p \to \phi\Lambda$ and finds a discrepancy of at least a factor of two.

30. S. L. Adler, Institute for Advanced Study preprint, 1968 (unpublished).

31. M. Braunschwieg et al., Phys. Letters 26B, 405 (1968).

32. F. J. Gilman, unpublished.

33. G. McClellan et al., Phys. Rev. Letters 22, 377 (1969).

34. F. Bulos et al., Phys. Rev. Letters 22, 490 (1969).

35. J. G. Asbury et al., Phys. Rev. Letters 19, 865 (1967); J. G. Asbury et al., Phys. Rev. Letters 20, 227 (1968).

36. J. E. Augustin et al., Phys. Letters 28B, 503 (1969).

37. S. C. C. Ting, rapporteur's talk in Proceedings of the Fourteenth International Conference on High Energy Physics, Vienna, Austria, 1968 (CERN Scientific Information Service, Geneva, Switzerland, 1968), p. 43.

38. M. Gell-Mann, D. Sharp and W. G. Wagner, Phys. Rev. Letters 8, 261 (1962).

39. N. Barash-Schmidt et al., Rev. Mod. Phys. 41, 109 (1969) and UCRL-8030.

40. See, for example, J. G. Cordes and P. J. O'Donnell, University of Toronto preprint, 1968 (unpublished); and J. W. Moffat, Phys. Rev. Letters 20, 620 (1968) and references therein.

41. S. J. Brodsky and J. Pumplin, preprint, SLAC-PUB-554, 1969 (unpublished); K. Gottfried and D. R. Yennie, preprint, 1969 (unpublished); M. Nauenberg, Phys. Rev. Letters 22, 556 (1969).

42. Y. Eisenberg et al., Phys. Rev. Letters 22, 669 (1969).

43. For the original definitions of W_1 and W_2 see S. D. Drell and J. D. Walecka, Ann. Phys. (N. Y.) 28, 18 (1964).

44. For a review of the kinematics and the connections between the cross sections and the invariant functions, see, for example, F. J. Gilman, Phys. Rev. 167, 1365 (1968).

45. J. D. Bjorken, preprint, SLAC-PUB-510, 1968 (unpublished).

46. E. D. Bloom et al. contributed paper 563 and W. K. H. Panofsky, rapporteur's talk in Proceedings of the Fourteenth International Conference on High Energy Physics, Vienna, Austria (CERN Scientific Information Service, Geneva, Switzerland, 1968), p. 23.

47. See, for example, J. D. Bjorken, "Current Algebra at Small Distances" Varenna School Lectures, Course XLI, Varenna, Italy (1967) and SLAC-PUB-338.

48. R. P. Feynman, unpublished.

49. J. D. Bjorken and E. Paschos, to be published.

50. H. Harari, Weizmann Institute preprint, 1968 (unpublished).

51. H. D. I. Abarbanel, M. L. Goldberger, and S. B. Treiman, Phys. Rev. Letters 22, 500 (1969).

52. S. D. Drell, D. J. Levy and T. M. Yan, preprint, SLAC-PUB-556, 1969 (unpublished).

53. J. J. Sakurai, University of Chicago preprint, 1969 (unpublished).

54. Some progress toward showing how the universal form might come out of ladder graph models in field theory has been made in Refs. 51 and 52. It is proposed in Ref. 53 that $\nu W_2(\nu, q^2)$ is not universal except in the limit $\nu^2 >> q^2 >> m_\rho^2$, so that one does not expect universality for $q^2 \simeq 1\,(\mathrm{GeV/c})^2$.

Figure Captions

Figure 1 - Summary of $\gamma + p \rightarrow$ pseudoscalar meson + baryon differential cross sections from Ref. 1.

Figure 2 - Differential cross sections at high energies for $\gamma + p \rightarrow \pi^+ + n$ from Ref. 2.

Figure 3 - Differential cross sections at high energies and small momentum transfers for $\gamma + p \rightarrow \pi^+ + n$ from Ref. 2.

Figure 4 - Effective value of the exchanged Regge spin $\alpha(t)$, from $d\sigma/dt \propto s^{2\alpha(t)-2}$ for the process $\gamma + p \rightarrow \pi^+ + n$.

Figure 5 - Comparison of the pion plus Regge cut (dashed curves) model with the "pseudomodel" (solid curves), from Ref. 4.

Figure 6 - Example of how the destructive interference of the "evasive" pion amplitude, B, and the Regge cut amplitude, A, can generate a forward peak in the net amplitude, M, from Ref. 9.

Figure 7 - Measurements of the π^-/π^+ ratio from photoproduction on deuterium at high energy, from Ref. 11.

Figure 8 - The ratio $\sum = \frac{\sigma_\perp - \sigma_\parallel}{\sigma_\perp + \sigma_\parallel}$ for the process $\gamma + p \rightarrow \pi^+ + n$ with polarized photons from C. Geweneger et al., Ref. 12.

Figure 9 - Summary of the measurements of Ref. 12 of $\sum = \frac{\sigma_\perp - \sigma_\parallel}{\sigma_\perp + \sigma_\parallel}$ for both π^+ and π^- photoproduction.

Figure 10 - Measurements of Ref. 14 of $d\sigma/dt$ for $\gamma + p \rightarrow \pi^0 + p$ at high energy.

Figure 11 - Polarized photon data at $k_\gamma^{lab} = 3$ GeV/c of Ref. 15 for $\gamma + p \rightarrow \pi^0 + p$.

Figure 12 - Differential cross sections for $\gamma + p \rightarrow \pi^- + \Delta^{++}$, from Ref. 19.

Figure 13 - Small momentum transfer differential cross sections for $\gamma + p \rightarrow \pi^- + \Delta^{++}$, from Ref. 19.

Figure 14 - Comparison[11, 20] of the VDM relation, Eq. (4), with experiment using $g^2_{\gamma\rho} = 4 \times 10^{-3}$.

Figure 15 - Comparison[22] of the VDM relation, Eq. (6), with experiment. The crosses are values for $A(\pi^+ + \pi^-)$ from photoproduction, and the circles are values for $\rho^{hel}_{1-1}/\rho^{hel}_{11}$ from $\pi^- p \rightarrow \rho^o n$.

Figure 16 - Comparison[26] of the first of Eqs. (5) with experiment, which is independent of rotations about the normal to the production plane. $\gamma^2_\rho/4\pi = 0.52$ was used in the comparison.

Figure 17 - Comparison[27] of the VDM model relation, Eq. (8), with experiment at 8 GeV/c.

Figure 18 - Observation[31] of the interference between the Primakoff effect (one photon exchange) and the rest of the amplitudes in π^o photoproduction. The solid curves are for constructive interference and the dashed curves for destructive interference.

Figure 19 - (a) Best fit (solid line) to the A dependence of the forward cross section for $\gamma + A \rightarrow \rho + A$ normalized to Cu, from Ref. 34. The best fit gives $\sigma_{\rho N} = 31 \pm 4$ mb.

(b) Values of $\gamma^2_\rho/4\pi$ deduced from measurements of the forward cross section for $\gamma + A \rightarrow \rho + A$ on various nuclei using $\sigma_{\rho N} = 31$ mb.

(c) Relation between $\gamma^2_\rho/4\pi$ and $\sigma_{\rho N}$ for various nuclei given the measured values of the forward cross section at SLAC[34].

Figure 20 - Table of values for $\gamma^2_\rho/4\pi$ deduced from different experiments and theoretical calculations, from Ref. 37.

Figure 21 - Prediction of the energy and A dependence of the photon-nucleus total photoabsorption cross sections assuming rho dominance, from Brodsky and Pumplin, Ref. 41.

Figure 22 - Plot of the 6^o data of Ref. 46 against $\omega = \nu/q^2$. $F(\omega) = \nu W_2(\nu, q^2)$ is plotted under the two assumptions $R = \sigma_T/\sigma_S$ equals infinity to zero.

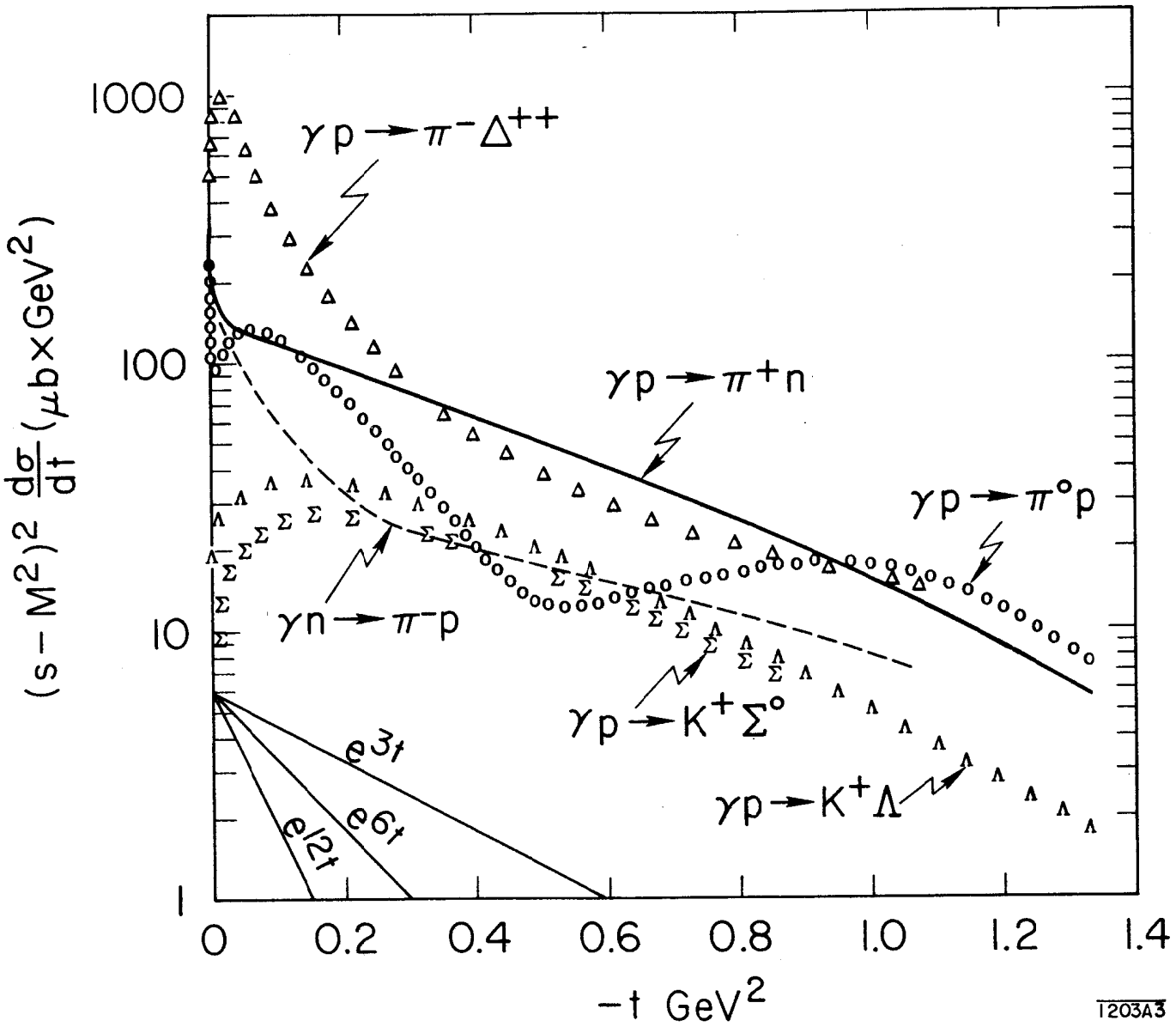
1000
100
10
1
$(s-M^2)^2 \frac{d\sigma}{dt}$ (μb×GeV^2)
$\gamma p \to \pi^- \Delta^{++}$
$\gamma p \to \pi^+ n$
$\gamma p \to \pi^\circ p$
$\gamma n \to \pi^- p$
$\gamma p \to K^+ \Sigma^\circ$
$\gamma p \to K^+ \Lambda$
e^{3t}
e^{6t}
$e^{t/2}$
0
0.2
0.4
0.6
0.8
1.0
1.2
1.4
$-t$ GeV^2
1203A3

Fig. 1

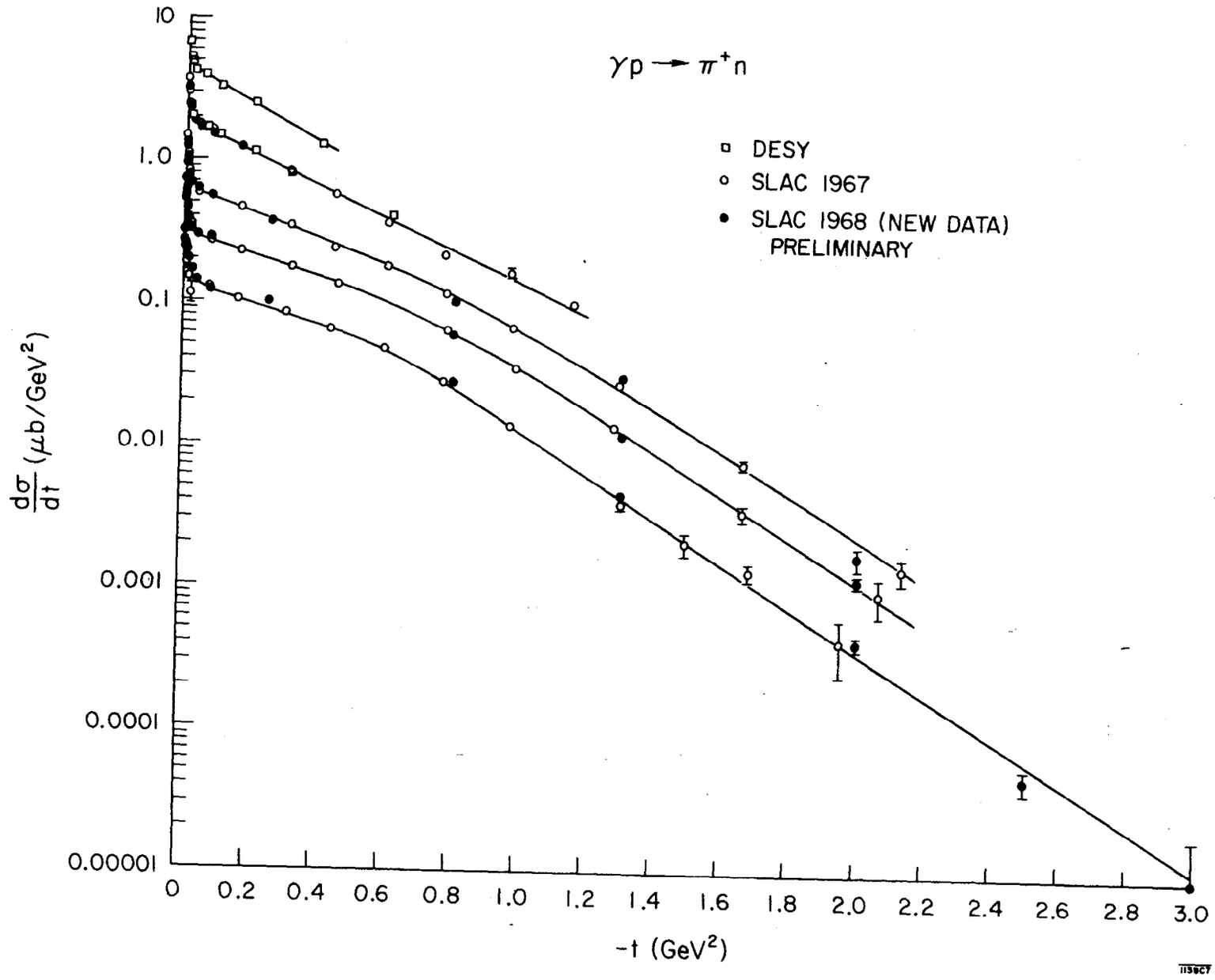
$\gamma p \rightarrow \pi^+ n$
DESY
SLAC 1967
SLAC 1968 (NEW DATA)
PRELIMINARY
$\frac{d\sigma}{dt}$ (μb/GeV^2)
10
1.0
0.1
0.01
0.001
0.0001
0.00001
0
0.2
0.4
0.6
0.8
1.0
1.2
1.4
1.6
1.8
2.0
2.2
2.4
2.6
2.8
3.0
-t (GeV^2)

Fig. 2

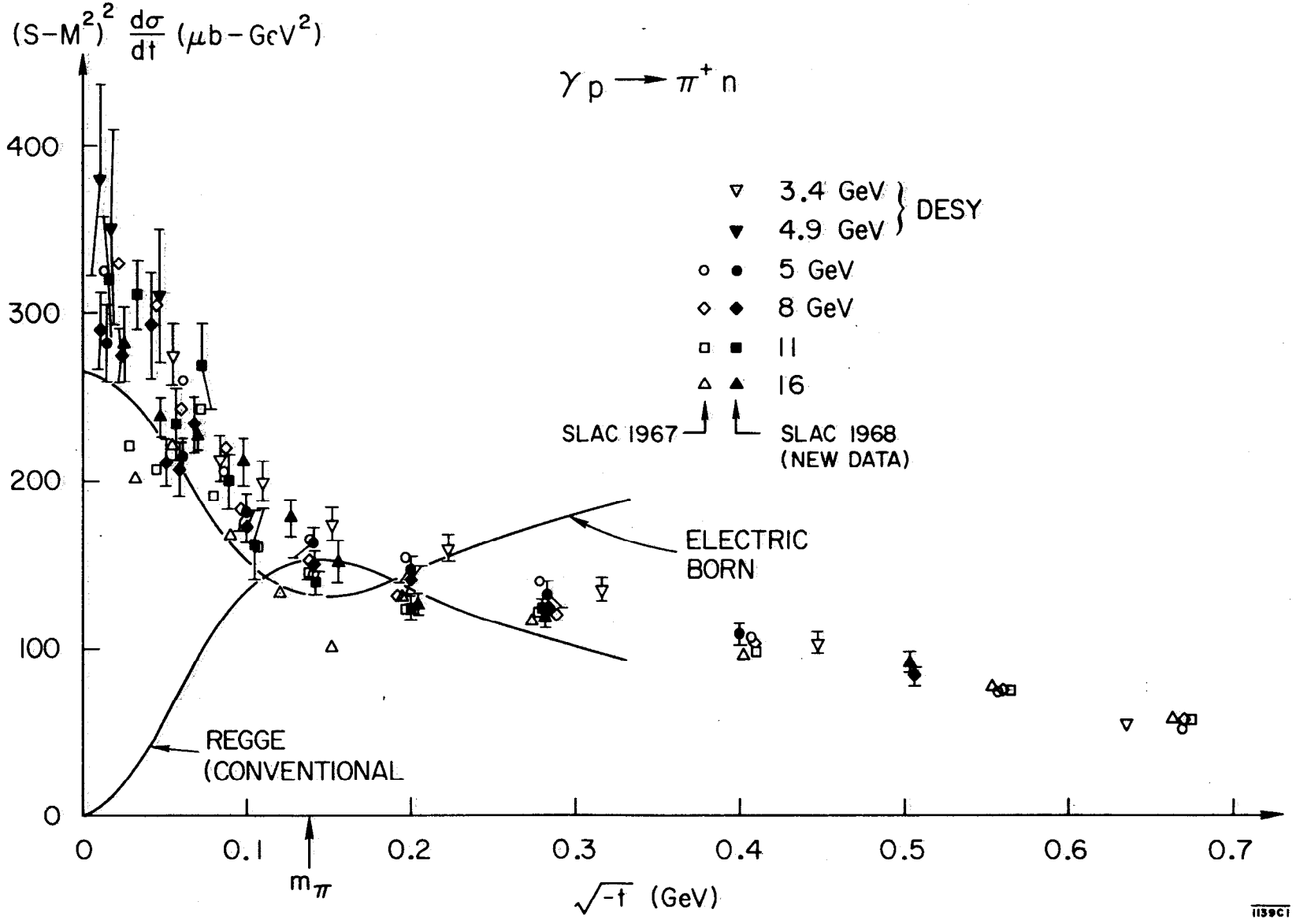
$(S-M^2)^2 \frac{d\sigma}{dt}$ ($\mu b - GeV^2$)
$\gamma p \rightarrow \pi^+ n$
400
300
200
100
0
3.4 GeV
4.9 GeV
DESY
5 GeV
8 GeV
11
16
SLAC 1967
SLAC 1968
(NEW DATA)
ELECTRIC
BORN
REGGE
(CONVENTIONAL
0
0.1
0.2
0.3
0.4
0.5
0.6
0.7
m_π
$\sqrt{-t}$ (GeV)
1139C1

Fig. 3

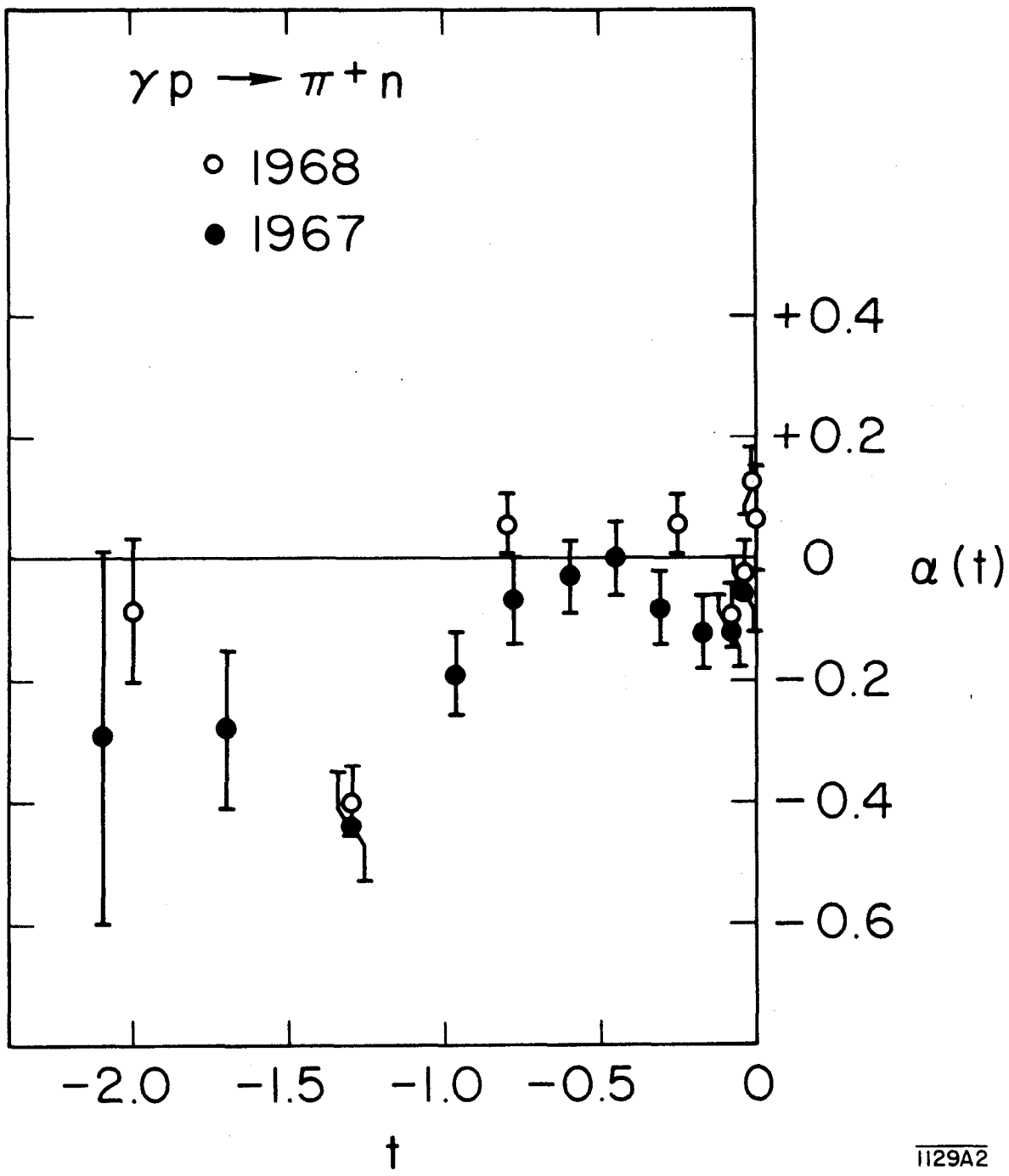

Fig. 4

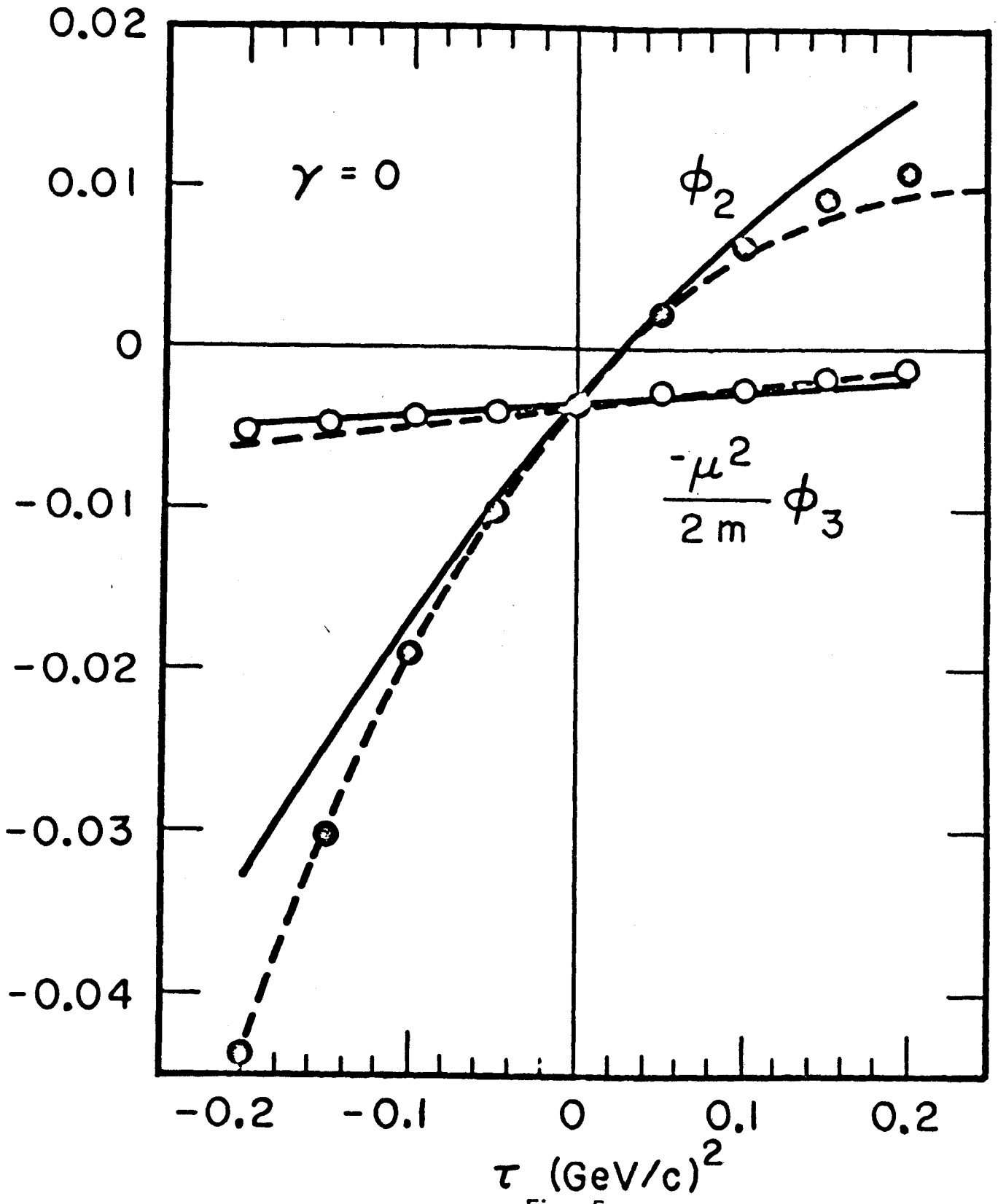
0.02
0.01
0
-0.01
-0.02
-0.03
-0.04
$\gamma = 0$
ϕ_2
$\frac{-\mu^2}{2m}\phi_3$
-0.2
-0.1
0
0.1
0.2
τ (GeV/c)^2

Fig. 5

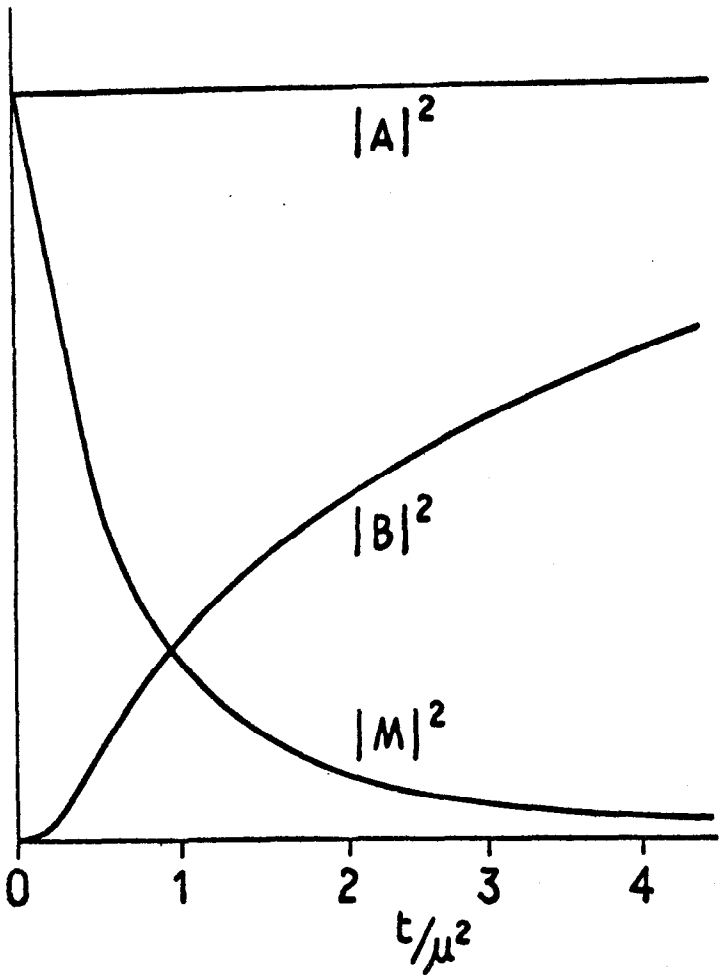

Fig. 6

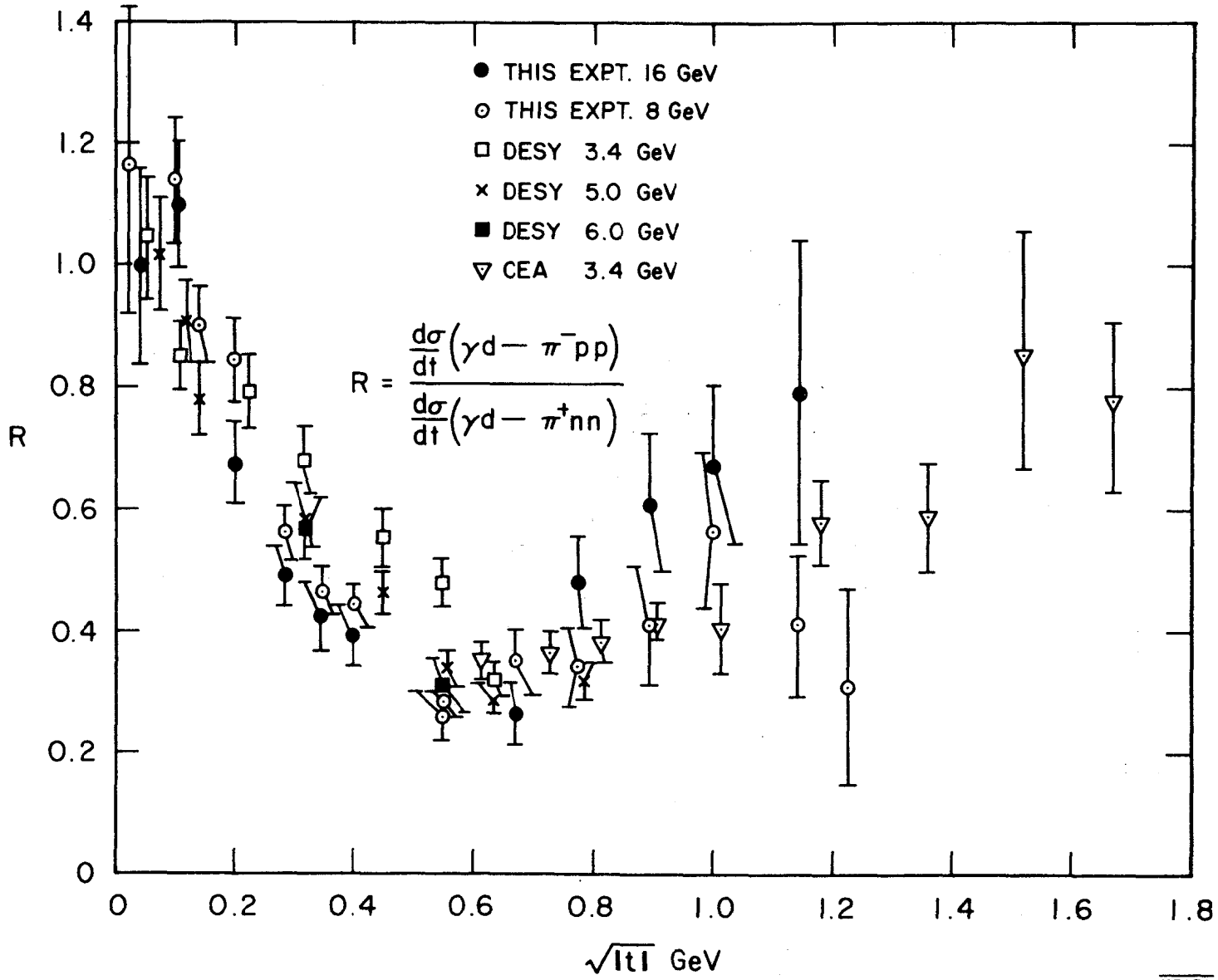
THIS EXPT. 16 GeV
THIS EXPT. 8 GeV
DESY 3.4 GeV
DESY 5.0 GeV
DESY 6.0 GeV
CEA 3.4 GeV
$R = \frac{\frac{d\sigma}{dt}(\gamma d - \pi^- pp)}{\frac{d\sigma}{dt}(\gamma d - \pi^+ nn)}$
R
$\sqrt{|t|}$ GeV
0
0.2
0.4
0.6
0.8
1.0
1.2
1.4
1.6
1.8
113983

Fig. 7

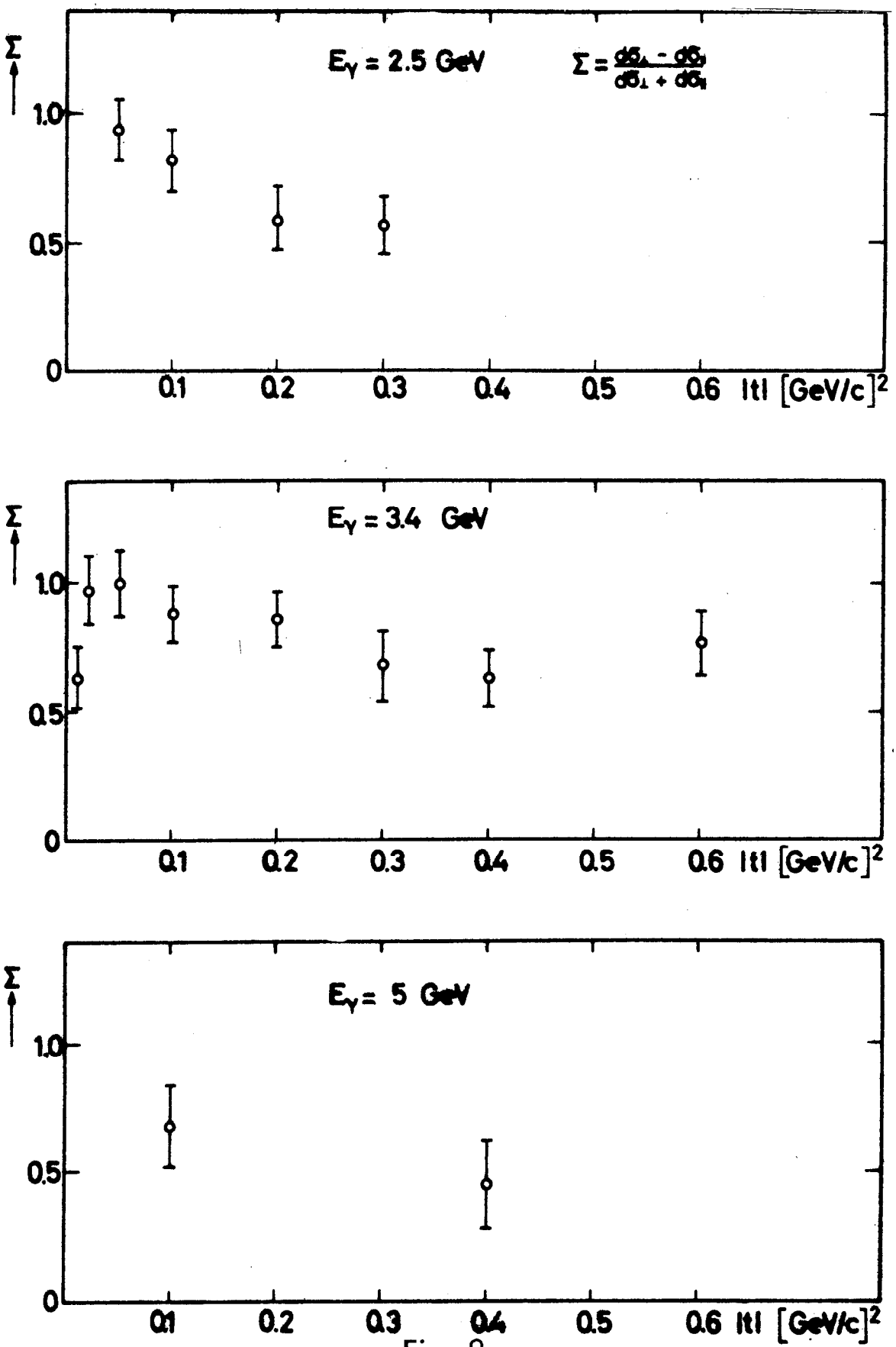
Σ
E_γ = 2.5 GeV
$\Sigma = \frac{d\sigma_\Delta - d\sigma_\parallel}{d\sigma_\perp + d\sigma_\parallel}$
1.0
0.5
0
0.1
0.2
0.3
0.4
0.5
0.6
|t| [GeV/c]^2
Σ
E_γ = 3.4 GeV
1.0
0.5
0
0.1
0.2
0.3
0.4
0.5
0.6
|t| [GeV/c]^2
Σ
E_γ = 5 GeV
1.0
0.5
0
0.1
0.2
0.3
0.4
0.5
0.6
|t| [GeV/c]^2

Fig. 8

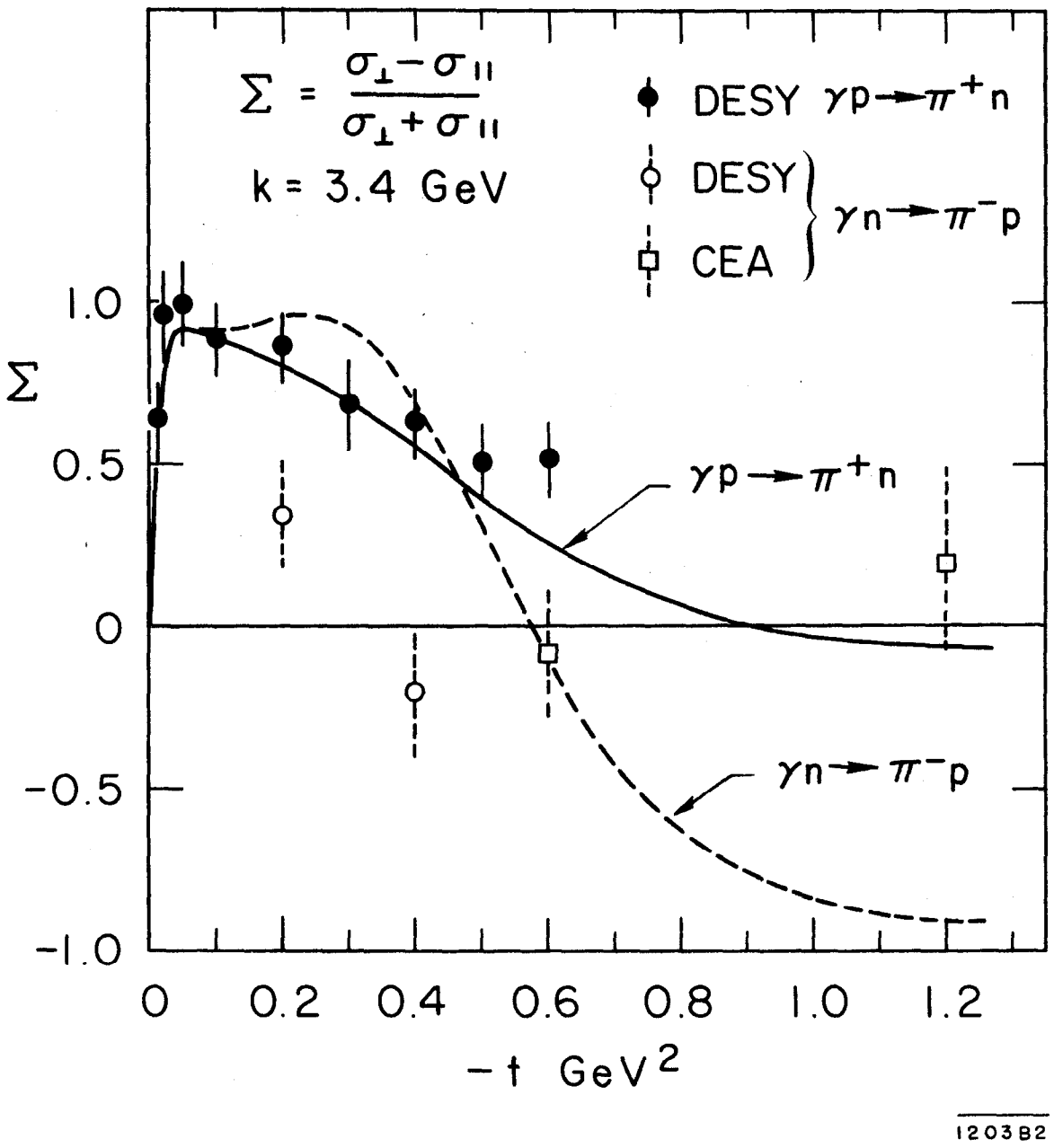
$\Sigma = \frac{\sigma_\perp - \sigma_{11}}{\sigma_\perp + \sigma_{11}}$
k = 3.4 GeV
DESY $\gamma p \to \pi^+ n$
DESY
CEA
$\gamma n \to \pi^- p$
$\gamma p \to \pi^+ n$
$\gamma n \to \pi^- p$
Σ
1.0
0.5
0
-0.5
-1.0
0
0.2
0.4
0.6
0.8
1.0
1.2
$-t$ GeV^2
1203B2

Fig. 9

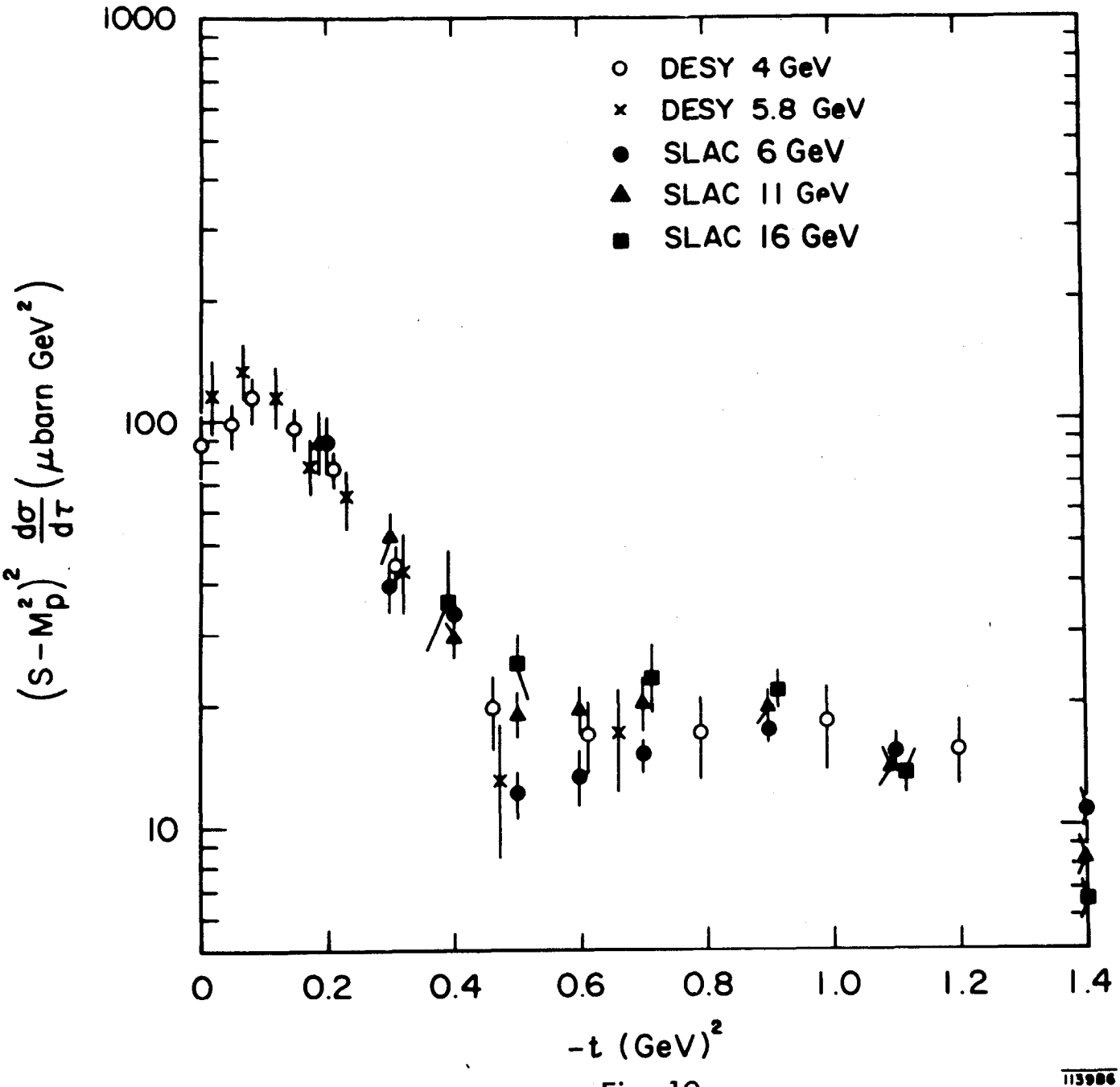
1000
100
10
0
0.2
0.4
0.6
0.8
1.0
1.2
1.4
DESY 4 GeV
DESY 5.8 GeV
SLAC 6 GeV
SLAC 11 GeV
SLAC 16 GeV
$(S-M_p^2)^2 \frac{d\sigma}{dt}$ (μbarn GeV^2)
$-t$ (GeV)^2
113986

Fig. 10

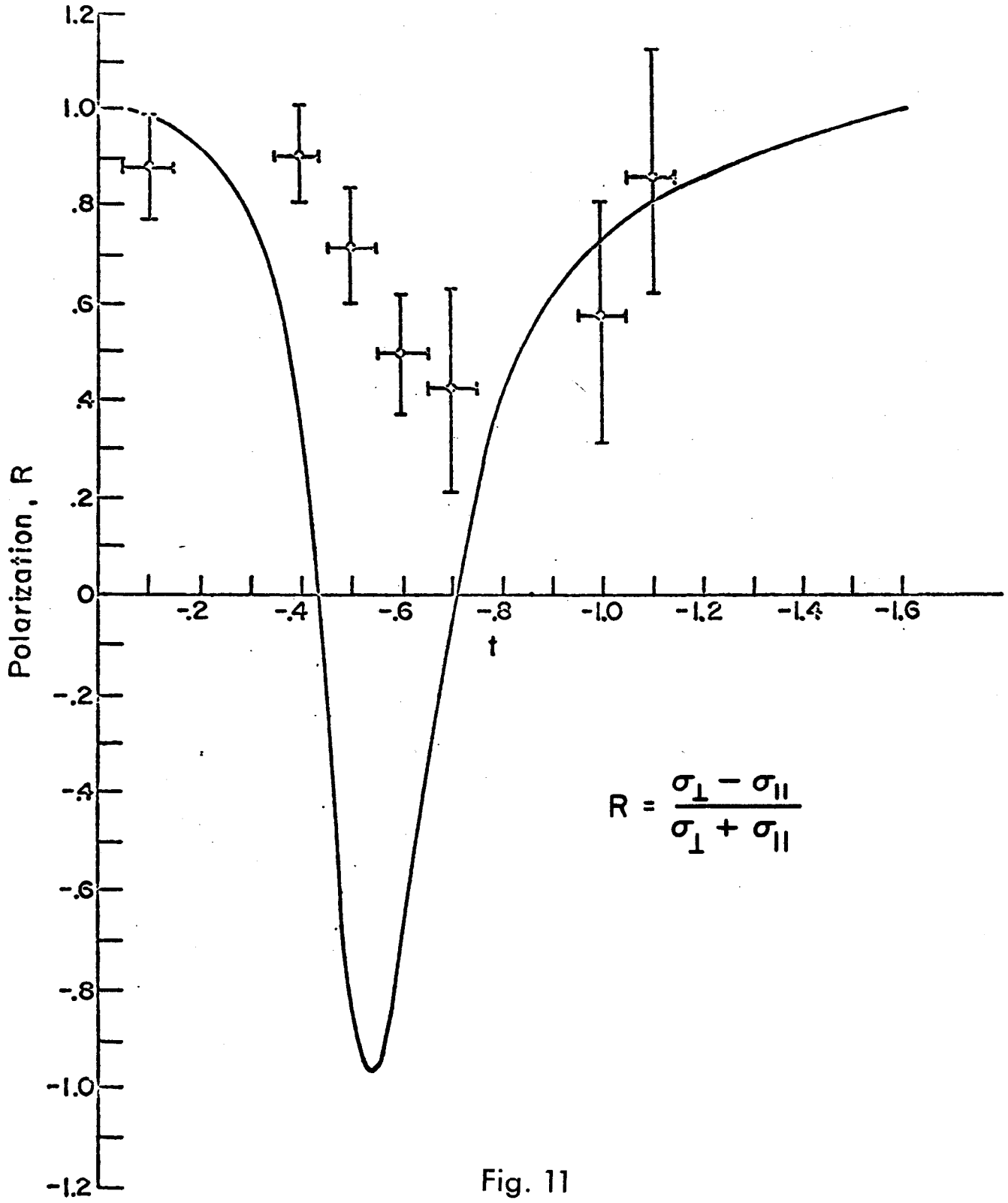
1.2
1.0
.8
.6
.4
.2
0
-.2
-.4
-.6
-.8
-1.0
-1.2
Polarization, R
-.2
-.4
-.6
-.8
-1.0
-1.2
-1.4
-1.6
t
$R = \frac{\sigma_\perp - \sigma_{||}}{\sigma_\perp + \sigma_{||}}$

Fig. 11

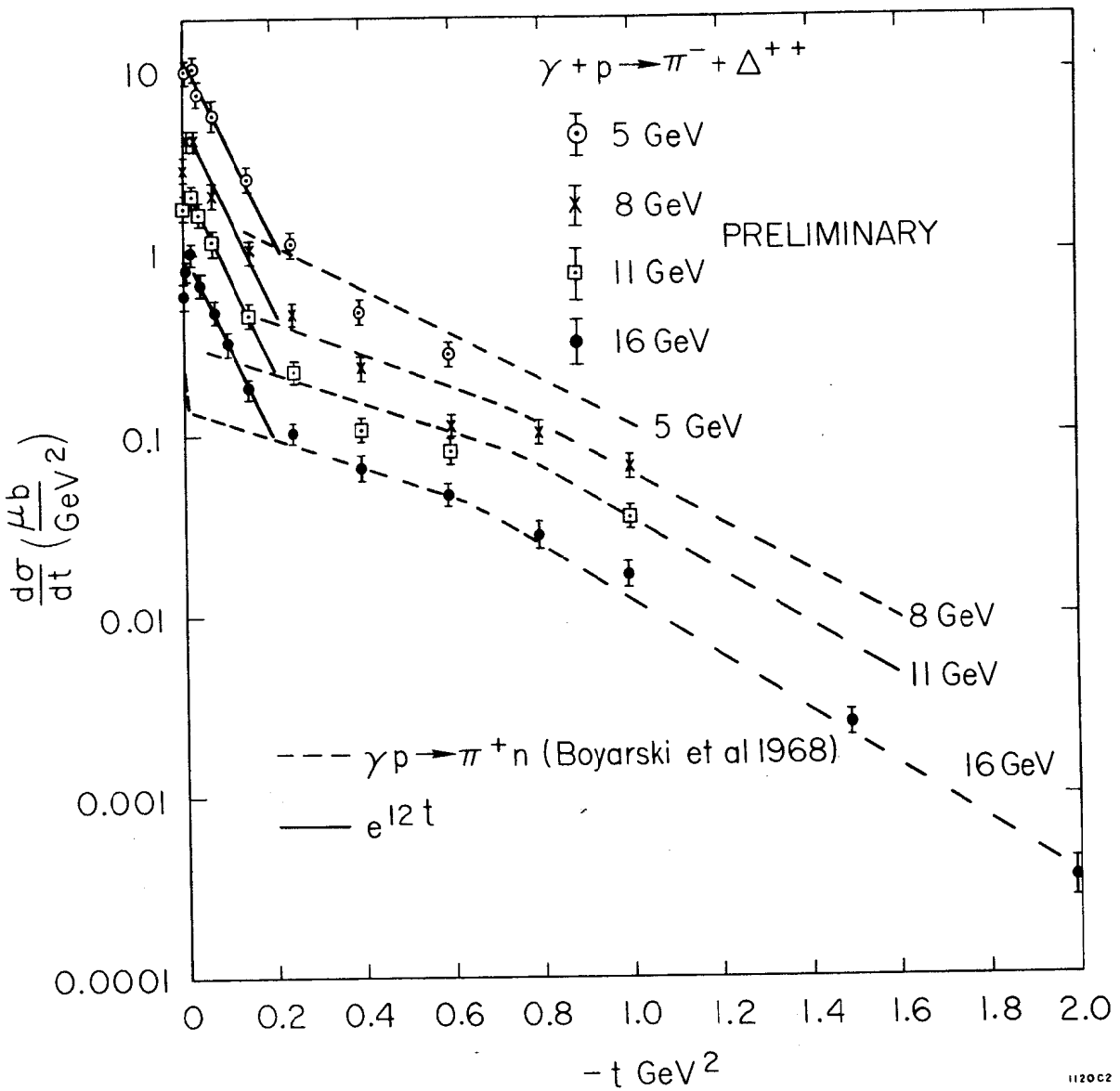
$\gamma + p \rightarrow \pi^- + \Delta^{++}$
5 GeV
8 GeV
11 GeV
16 GeV
PRELIMINARY
5 GeV
8 GeV
11 GeV
16 GeV
$\gamma p \rightarrow \pi^+ n$ (Boyarski et al 1968)
e^{12t}
$\frac{d\sigma}{dt}\left(\frac{\mu b}{GeV^2}\right)$
10
1
0.1
0.01
0.001
0.0001
0
0.2
0.4
0.6
0.8
1.0
1.2
1.4
1.6
1.8
2.0
$-t\ GeV^2$
1120C2

Fig. 12

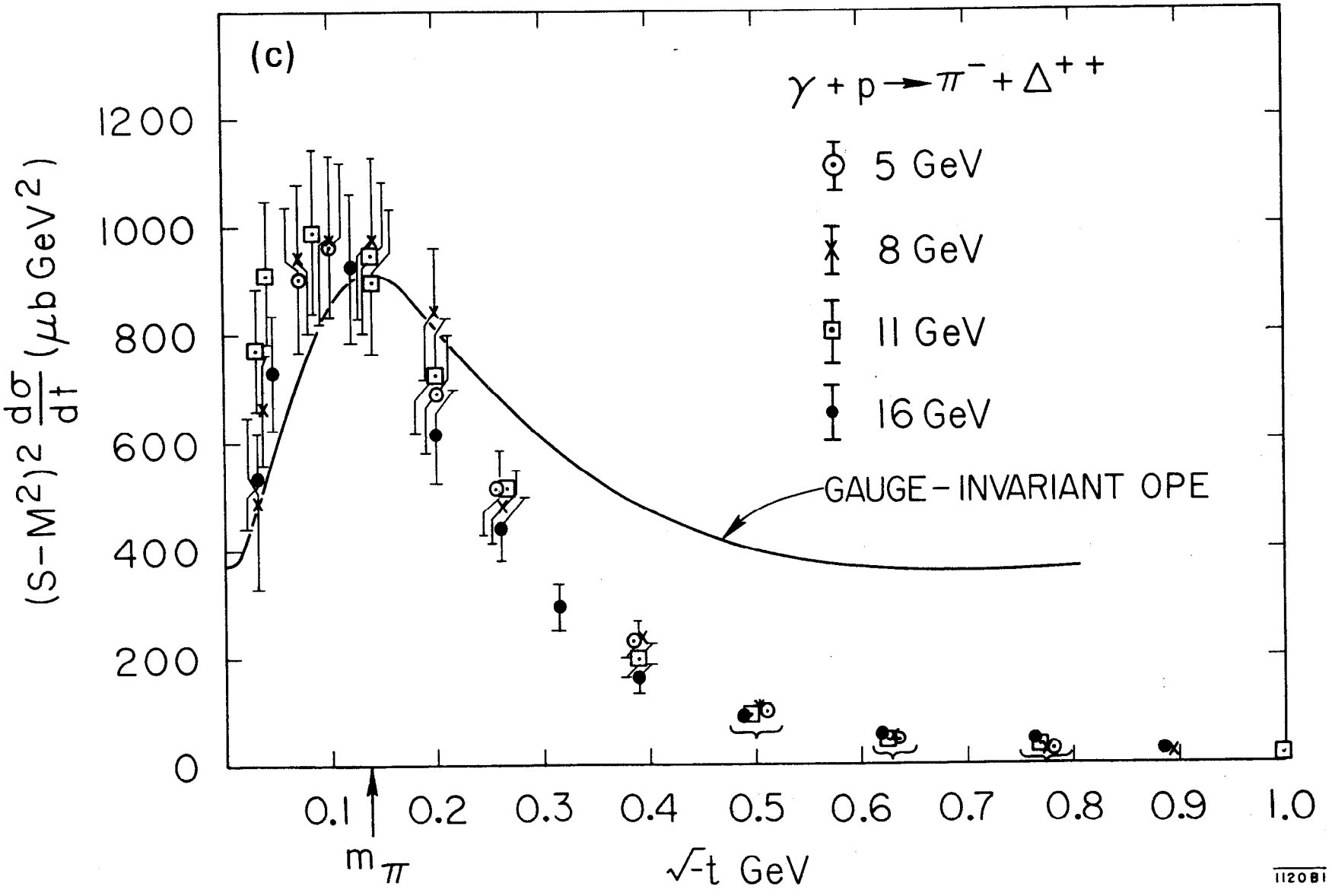
(c)
$\gamma + p \rightarrow \pi^- + \Delta^{++}$
5 GeV
8 GeV
11 GeV
16 GeV
GAUGE-INVARIANT OPE
$(S-M^2)^2 \frac{d\sigma}{dt}$ (μb GeV^2)
1200
1000
800
600
400
200
0
0.1
0.2
0.3
0.4
0.5
0.6
0.7
0.8
0.9
1.0
m_π
$\sqrt{-t}$ GeV
112081

Fig. 13

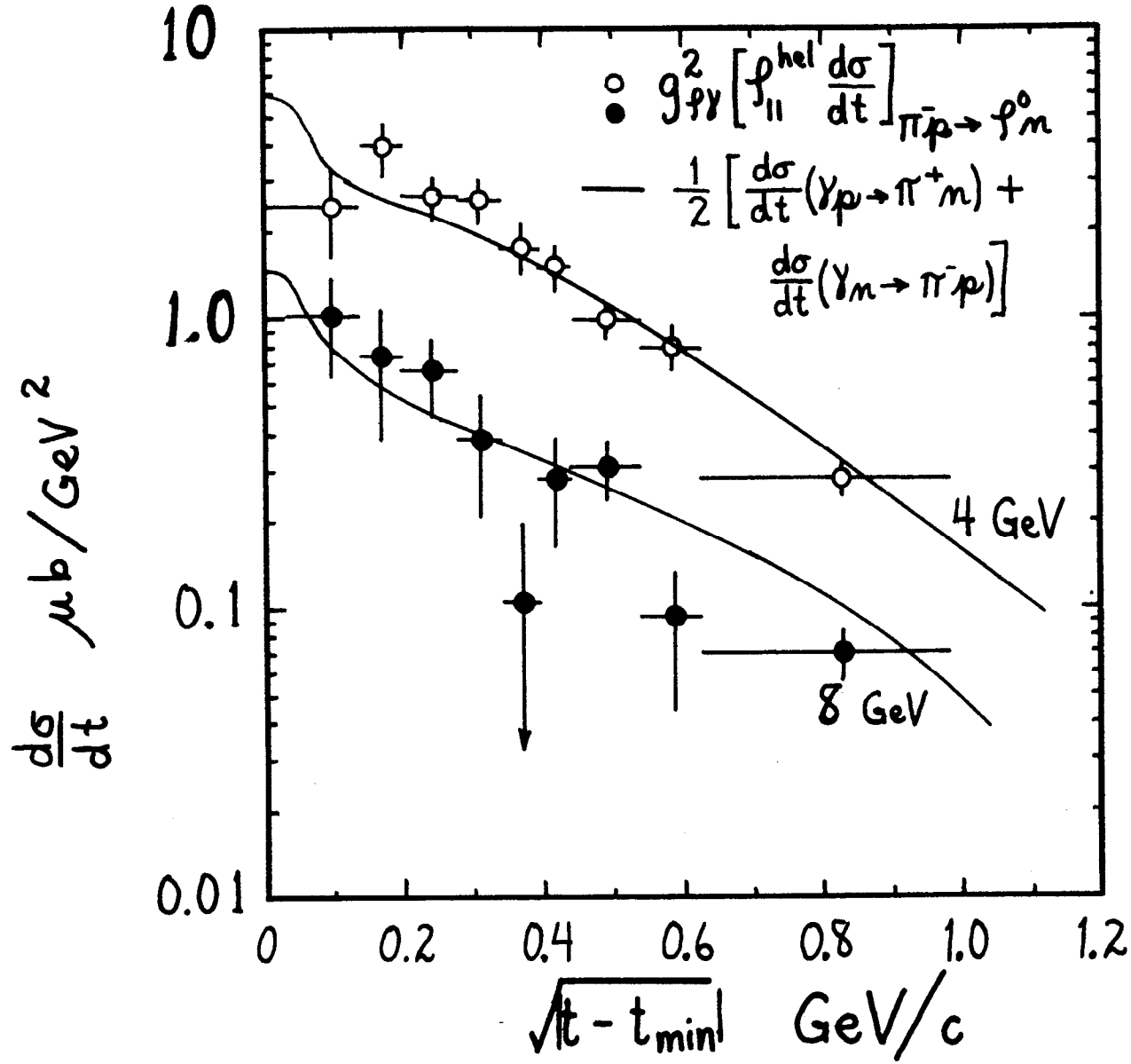
10
1.0
0.1
0.01
0
0.2
0.4
0.6
0.8
1.0
1.2
$\frac{d\sigma}{dt}$ μb/GeV^2
$\sqrt{|t - t_{min}|}$ GeV/c
$g^2_{\rho\gamma}\left[\rho^{hel}_{11}\frac{d\sigma}{dt}\right]_{\pi^-p\to\rho^0 n}$
$\frac{1}{2}\left[\frac{d\sigma}{dt}(\gamma p\to\pi^+ n) + \frac{d\sigma}{dt}(\gamma n\to\pi^- p)\right]$
4 GeV
8 GeV

Fig. 14

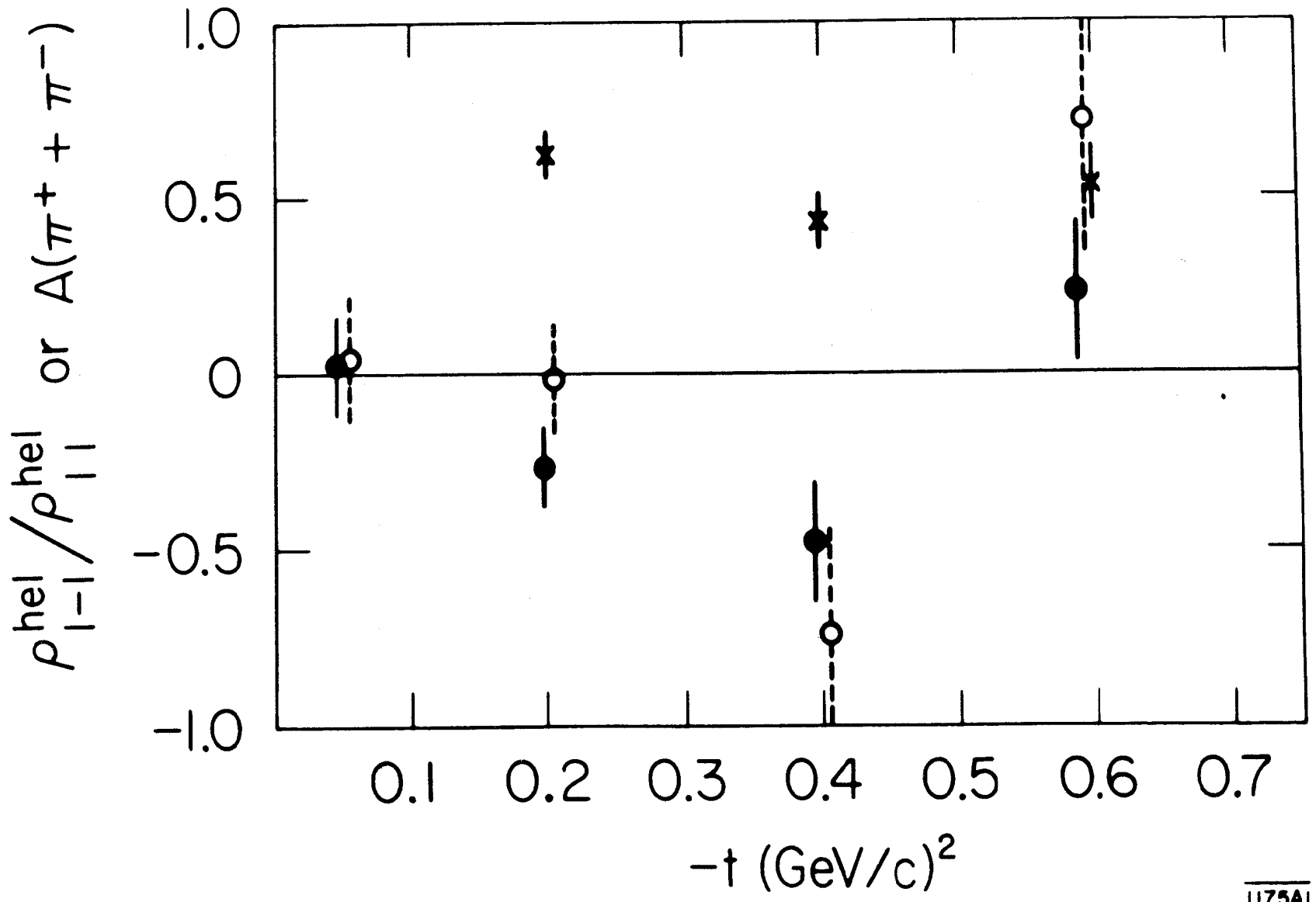
1.0
0.5
0
-0.5
-1.0
0.1
0.2
0.3
0.4
0.5
0.6
0.7
$\rho^{hel}_{1-1}/\rho^{hel}_{11}$ or $A(\pi^+ + \pi^-)$
$-t\ (GeV/c)^2$
1175A1

Fig. 15

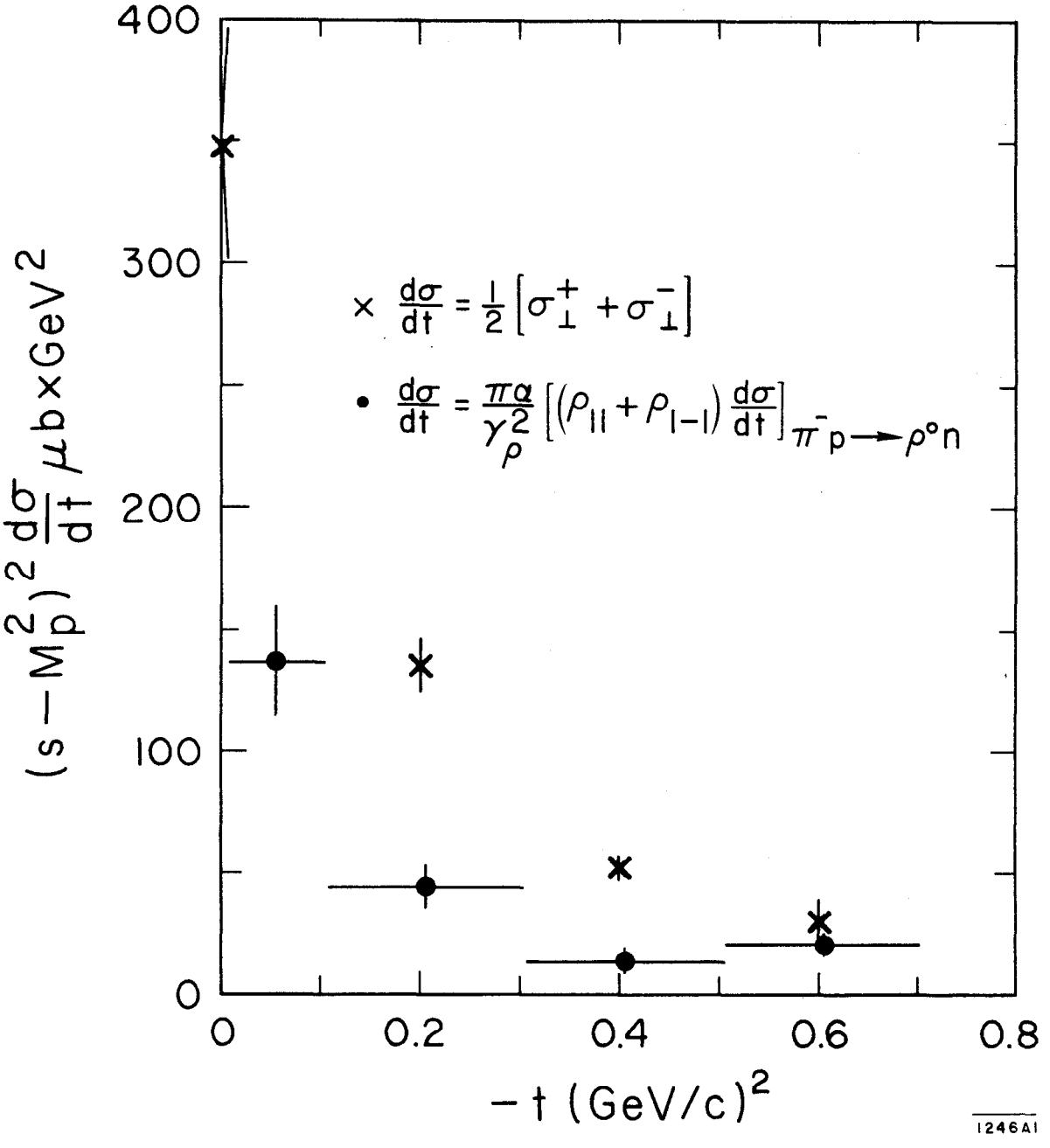
400
300
200
100
0
0
0.2
0.4
0.6
0.8
$(s-M_p^2)^2 \frac{d\sigma}{dt}\ \mu b \times GeV^2$
$-t\ (GeV/c)^2$
$\times\ \frac{d\sigma}{dt} = \frac{1}{2}\left[\sigma_\perp^+ + \sigma_\perp^-\right]$
$\bullet\ \frac{d\sigma}{dt} = \frac{\pi\alpha}{\gamma_\rho^2}\left[(\rho_{11}+\rho_{1-1})\frac{d\sigma}{dt}\right]_{\pi^- p \to \rho^0 n}$
1246A1

Fig. 16

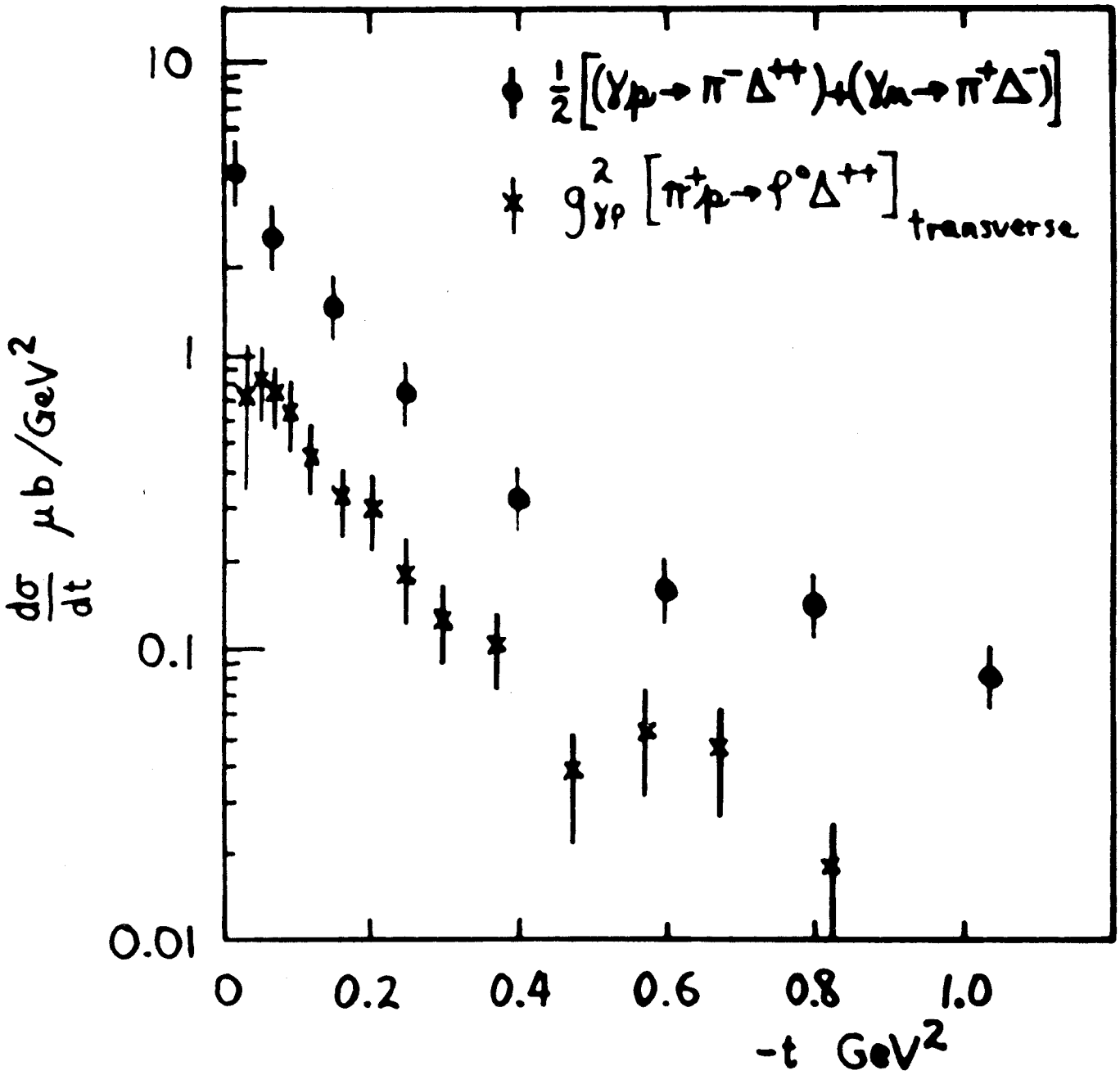
10
1
0.1
0.01
$\frac{d\sigma}{dt}$ μb/GeV^2
$\frac{1}{2}[(\gamma p \to \pi^- \Delta^{++}) + (\gamma n \to \pi^+ \Delta^-)]$
$g^2_{\gamma p}[\pi^+ p \to \rho^0 \Delta^{++}]_{\text{transverse}}$
0
0.2
0.4
0.6
0.8
1.0
$-t$ GeV^2

Fig. 17

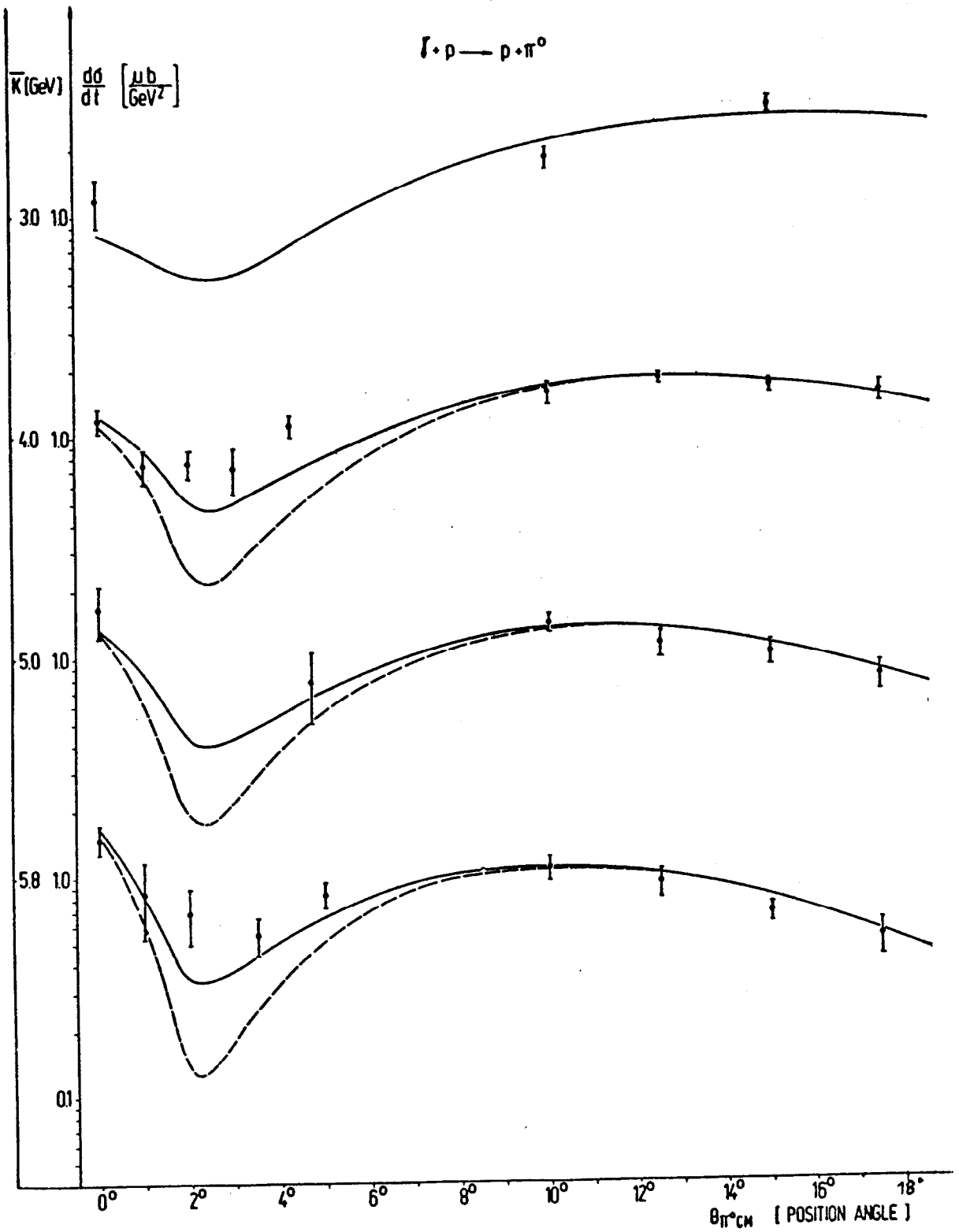
γ + p — p + π°
K̄ (GeV)
dσ/dt [μb/GeV²]
3.0 1.0
4.0 1.0
5.0 1.0
5.8 1.0
0.1
0°
2°
4°
6°
8°
10°
12°
14°
16°
18°
θπ°CM [POSITION ANGLE]

Fig. 18

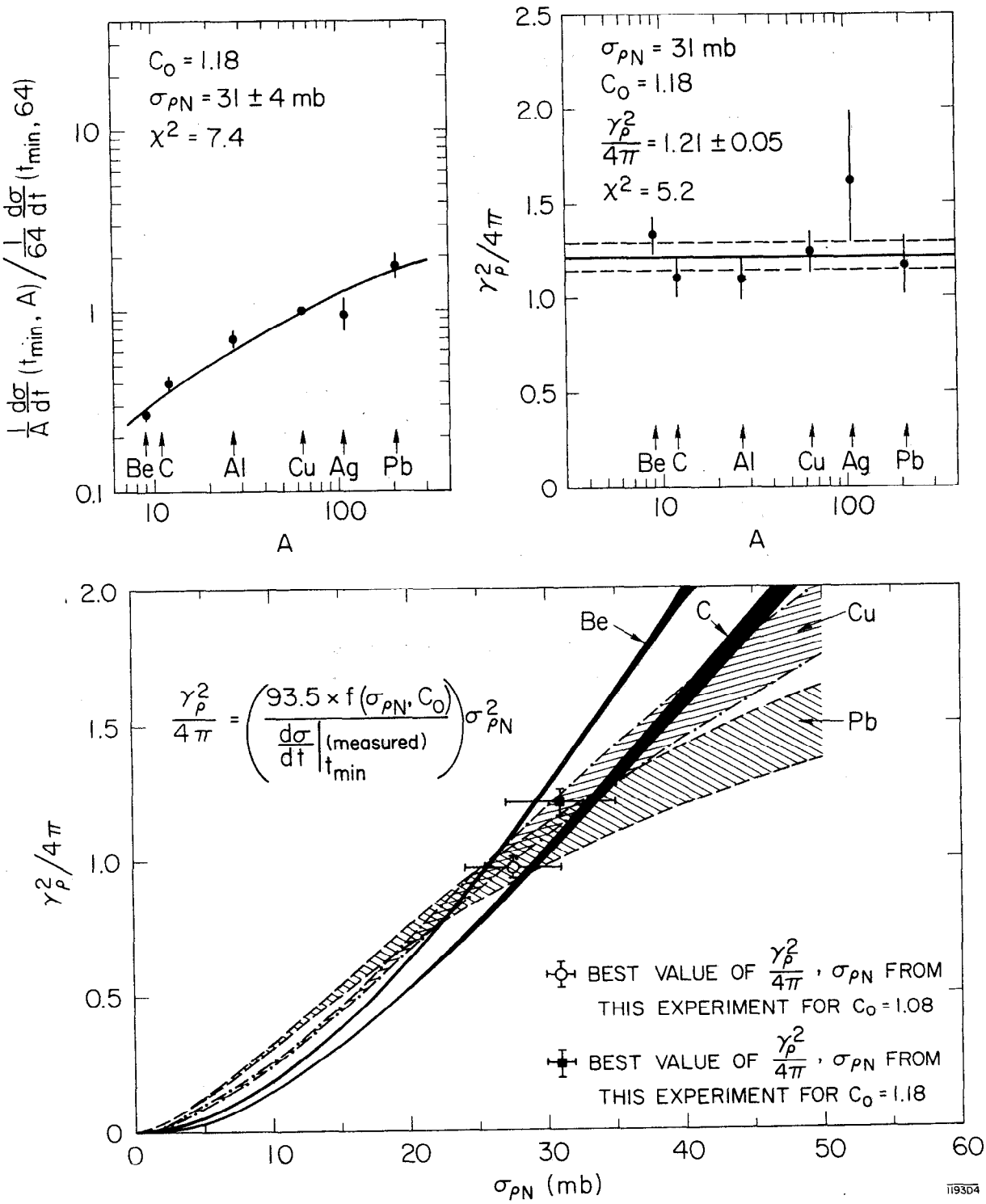
$C_0 = 1.18$
$\sigma_{\rho N} = 31 \pm 4$ mb
$\chi^2 = 7.4$
$\frac{1}{A}\frac{d\sigma}{dt}(t_{min}, A) / \frac{1}{64}\frac{d\sigma}{dt}(t_{min}, 64)$
Be C Al Cu Ag Pb
A
$\sigma_{\rho N} = 31$ mb
$C_0 = 1.18$
$\frac{\gamma_\rho^2}{4\pi} = 1.21 \pm 0.05$
$\chi^2 = 5.2$
$\gamma_\rho^2/4\pi$
$\frac{\gamma_\rho^2}{4\pi} = \left(\frac{93.5 \times f(\sigma_{\rho N}, C_0)}{\frac{d\sigma}{dt}\Big|_{t_{min}}(\text{measured})}\right)\sigma_{\rho N}^2$
Be
C
Cu
Pb
BEST VALUE OF $\frac{\gamma_\rho^2}{4\pi}$, $\sigma_{\rho N}$ FROM THIS EXPERIMENT FOR $C_0 = 1.08$
BEST VALUE OF $\frac{\gamma_\rho^2}{4\pi}$, $\sigma_{\rho N}$ FROM THIS EXPERIMENT FOR $C_0 = 1.18$
$\sigma_{\rho N}$ (mb)
1193D4

Fig. 19

Reactions	
p meson on mass shell $e^+ + e^- \rightleftarrows \rho^0$	$\gamma_\rho^2/4\pi$ $0.52 \begin{smallmatrix} + 0.07 \\ - 0.06 \end{smallmatrix}$
Photon on mass shell	$\gamma_\rho^2/4\pi$
1. $\sigma_T^2(\gamma p)/\frac{d\sigma}{dt}(\gamma p \to \rho^0 p)$	0.5 ± 0.1
2. π meson form factor	0.53 ± 0.04
3. $\gamma p \to \pi^+ n$, $\gamma n \to \pi^- p$ from 3 to 8 GeV	0.45 ± 0.10
4. π^+/π^- ratio from deuterium	0.45 ± 0.10
5. $d\sigma/dt\ (\gamma A \to \rho^0 A)_{C,Cu,Pb}$ DESY	0.5 ± 0.1
6. $\Gamma(\omega \to \pi\gamma)/\Gamma(\omega \to 3\pi)$	0.65 ± 0.10
7. $\frac{d\sigma}{dt}(\gamma p \to \pi^0 p)/\frac{d\sigma}{dt}(\pi N \to \rho N)$	~ 0.5
8. $\frac{d\sigma}{dt}(\gamma p \to \pi^+ n)$ versus $\frac{d\sigma}{dt}(\pi^- p \to \rho^0 n)$ [38]	0.45 (for this comparison see Fig. 21)
9. $d\sigma/dt\ (\gamma A \to \rho^0 A)$ Cornell	1.05 ± 0.20
Indirect measurements	
1. $\Gamma(\phi \to K^+K^-)$	$\gamma_\rho^2/4\pi$ equiv. $= 0.45 \pm 0.10$
2. $\Gamma(K^* \to K\pi)$ etc.	$\gamma_\rho^2/4\pi$ equiv. $= 0.6 \pm 0.1$

Fig. 20

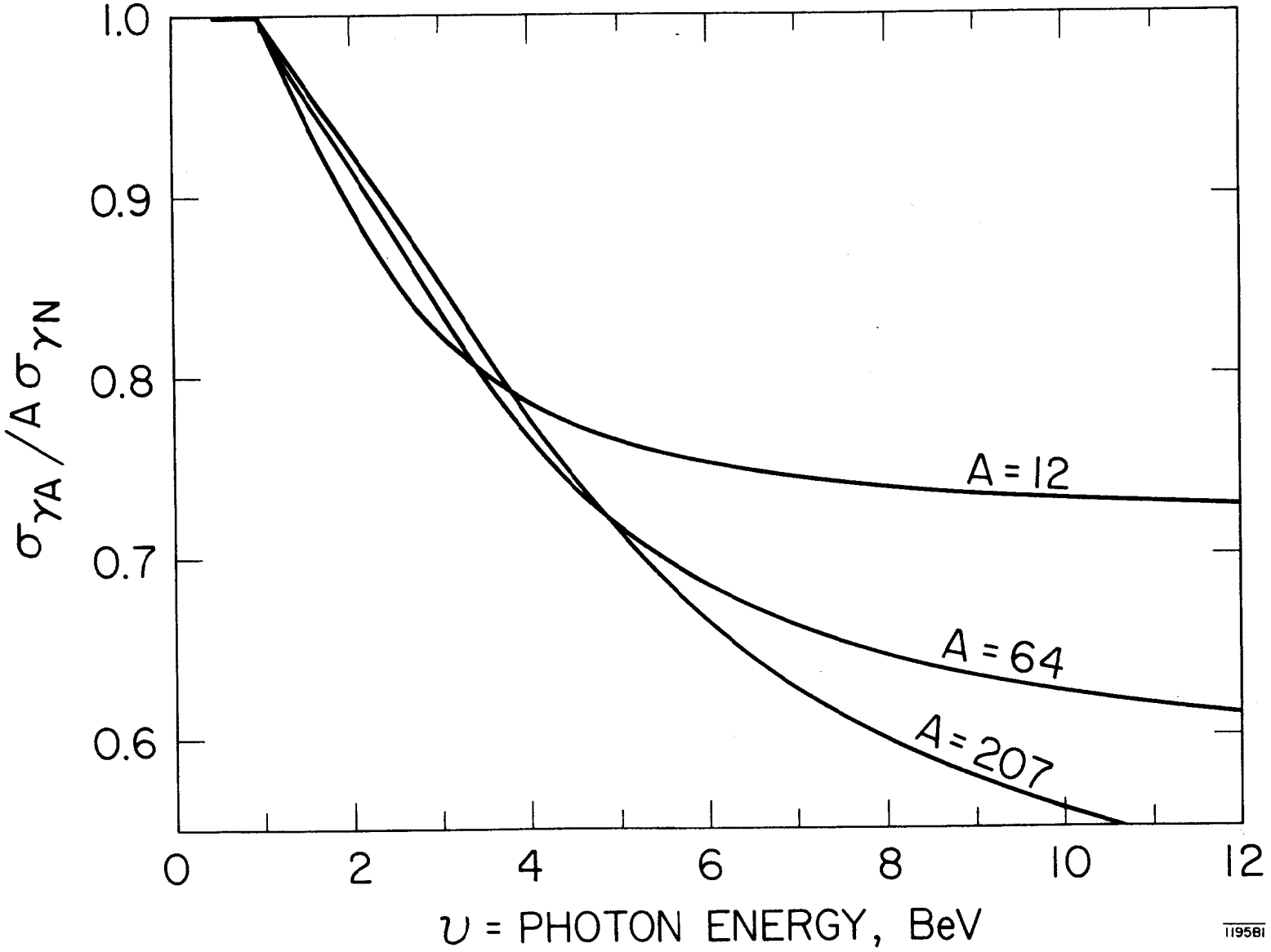
1.0
0.9
0.8
0.7
0.6
$\sigma_{\gamma A} / A \sigma_{\gamma N}$
A = 12
A = 64
A = 207
0
2
4
6
8
10
12
υ = PHOTON ENERGY, BeV
119581

Fig. 21

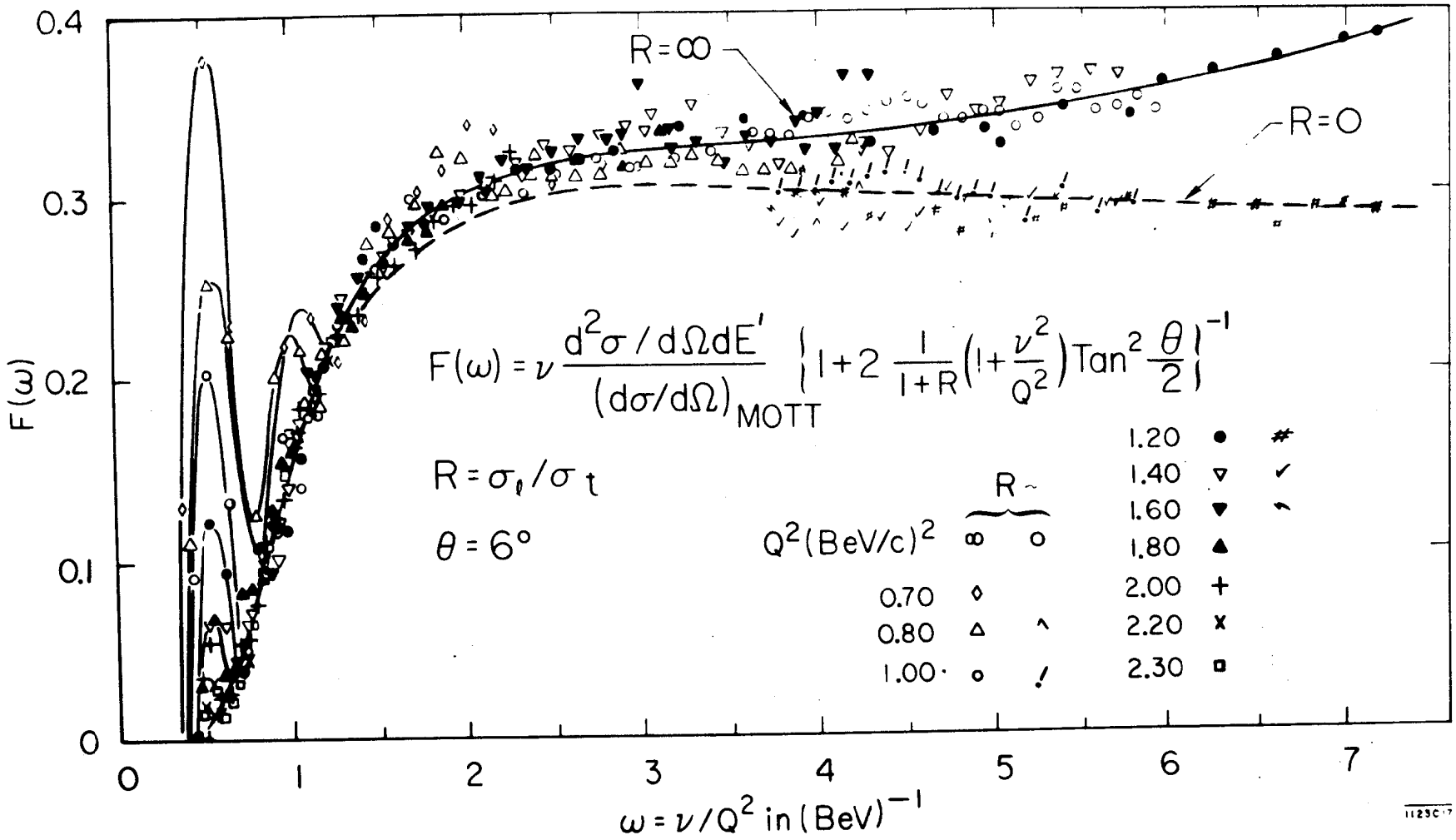
0.4
0.3
0.2
0.1
0
F(ω)
0
1
2
3
4
5
6
7
ω = ν/Q² in (BeV)⁻¹
R=∞
R=0
F(ω) = ν d²σ/dΩdE' / (dσ/dΩ)MOTT { 1+2 1/(1+R) (1+ν²/Q²) Tan² θ/2 }⁻¹
R = σl/σt
θ = 6°
R ~
Q²(BeV/c)²
∞
0
0.70
0.80
1.00
1.20
1.40
1.60
1.80
2.00
2.20
2.30
1129C17

Fig. 22